Effect of Magnetomechanical Coating on Beams with Varying Thickness

Author

SHOAIB NADEEM

00000117690

Supervisor

Dr. HASAN AFTAB SAEED

DEPARTMENT OF MECHANICAL ENGINEERING

COLLEGE OF ELECTRICAL & MECHANICAL ENGINEERING

NATIONAL UNIVERSITY OF SCIENCES AND TECHNOLOGY

ISLAMABAD

August, 2019

Effect of Magnetomechanical Coating on Beams with Varying Thickness

Author

SHOAIB NADEEM

00000117690

A thesis submitted in partial fulfillment of the requirements for the degree of

MS Mechanical Engineering

Thesis Supervisor:

Dr. HASAN AFTAB SAEED

Thesis Supervisor's Signature: _____

DEPARTMENT OF MECHANICAL ENGINEERING

COLLEGE OF ELECTRICAL & MECHANICAL ENGINEERING

NATIONAL UNIVERSITY OF SCIENCES AND TECHNOLOGY, ISLAMABAD

August, 2019

Declaration

I certify that this research work titled " *Effect of Magnetomechanical Coating on Beams with Varying Thickness"* is my own work. The work has not been presented elsewhere for assessment. The material that has been used from other sources it has been properly acknowledged / referred.

Signature of Student

SHOAIB NADEEM

2015-NUST-Ms-Mech-00000117690

Language Correctness Certificate

This thesis has been read by an English expert and is free of typing, syntax, semantic, grammatical and spelling mistakes. Thesis is also according to the format given by the university.

Signature of Student

SHOAIB NADEEM

2015-NUST-Ms-Mech-00000117690

Signature of Supervisor

Copyright Statement

Acknowledgements

I am greatly thankful to my Creator ALLAH Subhanaa-Wa-Tala, who directed me at every step of this work. You gave me inspiration, courage and wisdom to overcome difficulties which came across my way. I am also thankful to my loving parents for their never ending encouragement and support throughout my life and during preparation of this report.

I wish to express my profound gratitude and sincerest appreciation to my respected advisor **Dr. Hasan Aftab Saeed** for his support, guidance and ready assistance provided by him at all stages in the completion of this project report.

This work was not possible without full time support of **Mr. Imran Aziz,** who has been a great mentor and a source of inspiration to work in the area of vibration damping.

This is dedicated to my loving mother whose guidance and encouragement led me to this great achievement

Abstract

High cycle fatigue (HCF) caused by the vibratory stresses is the main cause of failure in rotating machine components, e.g. aircraft engine and gas turbine components. Which has lead to loss of millions of dollars. To avoid these kind of failures, vibrations must be reduced to an acceptable level, especially at resonant frequencies. A lot of previous studies have shown that coatings of different materials can significantly reduce these vibratory stresses by adding damping to the system. These include viscoelastic materials, plasma graded coatings, piezoelectric materials, and magneto-mechanical damping material coatings. But some of these have applicability and performance issues. Among these thin coatings, magneto-mechanical materials have shown to reduce vibratory stresses significantly. In this study, improvement in damping characteristics have been explored under different thicknesses of the magnetomechanical coatings. The effect of different structure thicknesses under same magneto-mechanical coating of 200μm is also studied. The experimental results are validated by numerical results by performing FEA analysis in MSC NASTRAN. The results show, increase in damping of the system by increasing the thickness of the magnetomechanical coating. And the magneto-mechanical coating of 200μm gives the best damping properties when applied to thin structure as compared to thick structures.

Key Words: *High cycle fatigue, Vibratory Stresses, Magneto-mechanical material coating.*

Table of Contents

Declaration ..... **i**
Language Correctness Certificate ..... **ii**
Copyright Statement ..... **iii**
Acknowledgements ..... **iv**
Abstract ..... **vi**
Table of Contents ..... **vii**
List of Figures ..... **ix**
List of Tables ..... **xi**
CHAPTER 1 : INTRODUCTION **1**
1.1 Background, Scope and Motivation 1
1.1.1 Magnetomechanical Damping 3
1.1.2 Mathematical Modeling of Magnetomechanical Damping 3
CHAPTER 2 : LITERATURE REVIEW **5**
CHAPTER 3 : EFFECT OF MAGNETOMECHANICAL COATING ON BEAMS OF DIFFERENT SIZES **11**
3.1 Experimental Work 11
3.1.1 Objective: 11
3.1.2 Beams 11
3.1.3 Coating 12
3.1.3.1 Coating Technique 13
3.1.4 Natural Frequencies 13
3.1.4.1 Instruments used 14
3.1.4.2 Experimental Work 16
3.1.5 Maximum Displacement 19
3.1.6 Damping Ratio 24
3.2 NUMERICAL ANALYSIS 28
3.2.1 Numerical Analysis Procedure 28
3.2.2 Modal Analysis 29
3.2.2.1 Natural Frequencies of beams 30
3.2.2.2 Mode Shapes of Uncoated Beams 32
3.2.3 Harmonic Response 35
3.3 Conclusion 43
CHAPTER 4 : EFFECT OF MAGNETOMECHANICAL COATING THICKNESS IN BEAM STRUCTURES **45**
4.1 Experimental Work 45
4.1.1 Natural Frequencies: 45

4.1.2 Maximum Displacement 47
4.1.3 Damping Ratio: 49
4.2 Numerical Analysis 51
4.2.1 Modal Analysis 51
4.2.1.1 Natural Frequencies of beams 51
4.2.2 Harmonic Response 52
4.3 Conclusion 59
REFERENCES 61

List of Figures

Figure 3-1: Beams manufactured for experimental analysis 12
Figure 3-2: Plasma Arc Coating method 13
Figure 3-3: Experimental setup for hammer tests....13
Figure 3-4: Accelerometer (B&K-4374) 14
Figure 3-5: Charge Amplifier B&K 2626....15
Figure 3-6: Vibration Analyzer SD 380 15
Figure 3-7: Setup to find Natural Frequencies....16
Figure 3-8: Comparison of 1st Natural Frequencies....17
Figure 3-9: Percentage Change in 1st Natural Frequencies....17
Figure 3-10: Natural Frequencies of 2mm Beam (Uncoated)....18
Figure 3-11: Natural Frequencies of 2mm Beam (Coated)....19
Figure 3-12: Shaker B&K 4808....21
Figure 3-13: Vibration Exciter Control B&K 1050....21
Figure 3-14: Comparison of Maximum Displacements at 1st Natural Frequencies....22
Figure 3-15: Percentage Change in Maximum Displacements....23
Figure 3-16: Maximum Displacement of 2mm Beam (Uncoated) at 1st natural frequency....23
Figure 3-17: Maximum Displacement of 2mm Beam (Coated) at 1st natural frequency....24
Figure 3-18: Comparison of Damping Ratios....26
Figure 3-19: Percentage Change in Damping Ratios....26
Figure 3-20: Time domain response of 2mm Beam (Uncoated) 27
Figure 3-21: Time domain response of 2mm Beam (Coated) 27
Figure 3-22: Flow Chart of Numerical Analysis Procedure 29
Figure 3-23: Beam for Modal Analysis....30
Figure 3-24: Comparison of 1st Natural Frequencies....31
Figure 3-25: Percentage Change in Natural Frequencies 31
Figure 3-26: 1st Natural Frequency (2mm-Uncoated beam)....32
Figure 3-27: 1st Natural Frequency (2mm-Coated beam)....32
Figure 3-28: 2nd Natural Frequency (2mm-Uncoated beam)....33
Figure 3-29: 2nd Natural Frequency (2mm-Coated beam)....33
Figure 3-30: 3rd Natural Frequency (2mm-Uncoated beam) 34
Figure 3-31: 3rd Natural Frequency (2mm-Coated beam) 34
Figure 3-32: Comparison of Von-Mises Stress at 1st Natural Frequencies....37
Figure 3-33: Comparison of Von-Mises Stress at 3rd Natural Frequencies 37
Figure 3-34: Comparison of Maximum Displacement at 1st Natural Frequencies....38
Figure 3-35: Comparison of Maximum Displacement at 3rd Natural Frequencies....38
Figure 3-36: Von-Mises Stress at 1st Natural Frequency (Uncoated beam)....39
Figure 3-37: Von-Mises Stress at 1st Natural Frequency (Coated beam)....39
Figure 3-38: Deformation Contours at 1st Natural Frequency (Uncoated beam) 40
Figure 3-39: Deformation Contours at 1st Natural Frequency (Coated beam) 40
Figure 3-40: Von-Mises Stress at 3rd Natural Frequency (Uncoated beam) 41
Figure 3-41: Von-Mises Stress at 3rd Natural Frequency (Coated beam) 41
Figure 3-42: Deformation Contours at 3rd Natural Frequency (Uncoated beam) 42
Figure 3-43: Deformation Contours at 3rd Natural Frequency (Coated beam) 42
Figure 3-44: Comparison of improvement in Vibration Parameters....44
Figure 4-1: Natural Frequencies of Beam (beam with 0.3mm Coating)....46
Figure 4-2: 1st Natural Frequencies of Beams 47
Figure 4-3: Maximum Displacement of Beam (beam with 0.3mm Coating) 48
Figure 4-4: Maximum Displacement in Beams....49
Figure 4-5: Time domain response of Beam (with 0.3mm Coating) 50
Figure 4-6: Damping Ratios of Beams 51
Figure 4-7: Comparison of 1st Natural Frequencies with Different Coating Thicknesses 52

Figure 4-8: Comparison of Von-Mises Stresses at 1st Natural Frequencies 55
Figure 4-9: Comparison of Von-Mises Stresses at 3rd Natural Frequencies.....55
Figure 4-10: Comparison of Maximum Displacements at 1st Natural Frequencies.....56
Figure 4-11: Comparison of Maximum Displacements at 3rd Natural Frequencies 56
Figure 4-12: Von-Mises Stress at 1st Natural Frequency (beam with 0.5mm Coating).....57
Figure 4-13: Von-Mises Stress at 3rd Natural Frequency (beam with 0.5mm Coating).....57
Figure 4-14: Deformation Contours at 1st Natural Frequency (beam with 0.5mm Coating) 58
Figure 4-15: Deformation Contours at 3rd Natural Frequency (beam with 0.5mm Coating).....58
Figure 4-16: Comparison of improvement in Vibration Parameters.....60

List of Tables

Table 3-1: Beam Properties 11
Table 3-2: Chemical Composition of Coating 12
Table 3-3: Coating Material Properties 12
Table 3-4: Sensor Settings for determination of natural frequency 14
Table 3-5: Charge Amplifier Settings for determination of natural frequency 14
Table 3-6: Vibration Analyzer settings for determination of natural frequency 15
Table 3-7: Natural Frequencies of Beams 16
Table 3-8: Sensor Settings for determination of maximum displacement 20
Table 3-9: Charge Amplifier Settings for determination of maximum displacement 20
Table 3-10: Vibration Analyzer settings for determination of maximum displacement 20
Table 3-11: Shaker details and settings for determination of maximum displacement 20
Table 3-12: Vibration Exciter Control settings for determination of maximum displacement 20
Table 3-13: Maximum Displacement of beams at 1st Natural Frequencies 22
Table 3-14: Sensor Settings for damping ratio measurement 25
Table 3-15: Charge Amplifier Settings for damping ratio measurement 25
Table 3-16: Vibration Analyzer settings for damping ratio measurement 25
Table 3-17: Damping Ratios of Beams 25
Table 3-18: Natural Frequencies of Uncoated and Coated beams 30
Table 3-19: Von-Mises Stresses at 1st Natural Frequencies 35
Table 3-20: Maximum Displacement at 1st Natural Frequency 35
Table 3-21: Von-Mises Stresses at 3rd Natural Frequencies 36
Table 3-22: Maximum Displacement at 3rd Natural Frequency 36
Table 3-23: Comparison of improvement in Vibration Parameters 43
Table 4-1: Natural Frequencies of beams 45
Table 4-2: Maximum Displacement of beams at 1st Natural Frequencies 47
Table 4-3: Damping Ratios of Beams 49
Table 4-4: Natural Frequencies of beams 51
Table 4-5: Von-Mises Stresses at 1st Natural Frequencies 53
Table 4-6: Maximum Displacement at 1st Natural Frequency 53
Table 4-7: Von-Mises Stresses at 3rd Natural Frequency 54
Table 4-8: Maximum Displacement at 3rd Natural Frequency 54
Table 4-9: Comparison of improvement in Vibration Parameters 59

CHAPTER 1 : INTRODUCTION

1.1 Background, Scope and Motivation

Most of the modern load carrying rotating machines (e.g. gas turbines and aircraft engine components) operate under severe loading conditions, and high cycle fatigue is the most common source of failure in these equipment. To avoid this, lifetime failure free criteria design by Goodman diagram or minor's rule is adopted. But, in reality these components often fail under severe operating conditions, because the design of these components doesn't take into account the degradation of material, scatter in experimental test data and uncertainties in actual loads. As a consequence, a number of failures have occurred especially in blading system of aircraft engines and these failures have resulted in loss of equipment worth millions of dollars.

High cycle fatigue causes blade failures, which increases inspection and maintenance costs and decreases operational readiness. The failure due to HCF occurs due to large vibratory stresses induced at resonance frequencies of the blades. The blades are designed such that their operational frequency don't match with their natural frequencies, but resonance can't be avoided at startups and shutdowns, because blades have to pass through natural frequencies to reach operational speed. Additionally as the aerodynamic loading varies during flight, and some of the aerodynamic loads can excite the blades at their natural frequencies. To avoid fatigue failures, we have to attenuate the maximum vibratory stresses at resonance to an acceptable level at resonance.

Adding damping to the system has been the most successful method of vibration suppression, different methods have been used by investigators to provide extra damping through blade dampers [1]. However, these dampers have some limitations in real world applications because they reduce vibrations by using motion of the components relative to each other, which causes energy dissipation through friction. Therefore, these dampers work effectively only for high displacements under low frequency vibration modes, and are not that effective for high frequency modes for which displacements are relatively small, especially in high stripe modes, where displacements are very small near the blade base. Additionally, as new blade designs don't have shrouds to improve their aerodynamics, so installation of these friction dampers is also a problem.

Due to negligible friction and aerodynamic damping at high frequency modes, most of the damping has to be provided by material damping. Numerous techniques have been used so far to increase material damping of the system. For example, viscoelastic damping materials have been integrated into rotating blades to reduce vibratory stresses under high frequency modes [2,3]. These viscoelastic materials are integrated by inserting their patches into milled cavities, and then sealing the cavities with cover sheet to restore the original airfoil contour. The damping is achieved by high internal friction of the viscoelastic material. However, this internal layer constrained damping method is not used widely, because the viscoelastic material creeps under high vibratory loads, and it also has temperature limitations.

Another damping method was introduced by Hoffman [4], this method uses three types of electromagnets embedded near the tip of the blade. These electromagnets are controlled and powered by an electronics module. These electromagnets are turned on when system is passing through a resonance frequency, the damping is achieved by dissipation of energy through eddy current caused by the magnetic fields introduced by electromagnets. This method has same manufacturing and temperature limitations as viscoelastic dampers.

From practical point of view, a high damping surface coating layer method is most suitable for vibration suppression. For this purpose, several materials, for example molybdenum, magnesium aluminate, and Hastelloy-X have been used as graded plasma coatings to accomplish high structural damping [5]. The coating has an outermost layer of an oxide ceramic, a middle layer made from a combination of one of the above mentioned alloys, and a material forming the upper layer. However, use of these plasma graded coatings is still not tested under high temperature and high frequency modes.

Some other damping techniques such as shunted piezoelectric damping, plasma sprayed ceramic coatings, self-tuning impact dampers and shape memory alloys have been used by researchers to suppress vibrations. But due to extreme engine environments, implementation of these methods is difficult, and they are yet to be employed in real aircraft engines.

The most effective and practical coating for vibration suppression is magnetomechanical coating, and it has been used by many researchers to control vibrations.

1.1.1 Magnetomechanical Damping

Magnetomechanical damping is produced by the irreversible rotation of the magnetic domain walls, caused by the stresses, against internal stress barrier of the material [6]. Domain theory [7] explains that ferromagnetic materials are made up of randomly oriented magnetic domains when it's in un-magnetized state. When external loading is applied, these domain walls of magnetic material move and try to line up in the direction of strain or stress, which in turn causes a higher magnetic field. And upon removal, the magnetic domain walls reorient themselves by rotating to a configuration with a lower magnetic field strength. This motion of domain walls causes magnetostrictive strain, and during this motion, energy of applied loading is lost over time, which causes vibration damping.

1.1.2 Mathematical Modeling of Magnetomechanical Damping

Smith and Birchak [8] linked the critical stress with average internal stress opposing the motion of magnetic domain boundaries. They distributed energy density dissipation per cycle in two different stress ranges:

$$\Delta Uc = \frac{K\lambda\sigma^3}{\sigma_{loc}^2} \quad \text{if} \quad \sigma < \sigma_{cr} \tag{1.1}$$

$$\Delta Uc = K\lambda\sigma_{loc} \quad \text{if} \quad \sigma > \sigma_{cr} \tag{1.2}$$

Where K is a constant which depends on the profile of hysteresis loop, λ is magnetostriction at saturation, σ is vibratory stress, σ_{loc} is internal local stress barrier, and σ_{cr} is the stress when the irreversible rotation of magnetic domain walls is saturated.

From Equations 1.1 and 1.2, the energy dissipation continually increases with increase in vibratory stress as K, σ_{loc} and λ are constants. However, it becomes constant after reaching a saturation point, which tells us that the magnetic domains have achieved their maximum possible magnetic field strength. To sum up the individual contributions from these two different regions, a probabilistic distribution function is given as follows:

$$N(\sigma) = \left(\frac{4}{\sigma_i^2}\right)\sigma e^{\frac{-2\sigma}{\sigma_i}} \tag{1.3}$$

By using this function, smith and birchak [9] remodeled the energy dissipation functions given in equations 1.1 and 1.2 to formulate a single energy dissipation density function as:

$$\Delta U_c = K\lambda\sigma_i\{1 - e^{-2s}(1 + 2s + 2s^2)\} \tag{1.4}$$

Where σ_i is the average internal stress, and s is defined as

$$\mathcal{S} = \frac{\sigma}{\sigma_i} = \frac{\varepsilon}{\varepsilon_i} \tag{1.5}$$

The lost factor of the coating is given by the following expression:

$$\eta_c = \frac{\Delta U_c}{2\pi U_c} \tag{1.6}$$

Because strain energy is

$$U_c = \frac{\sigma^2}{2E} \tag{1.7}$$

So the loss factor can be defined as:

$$\eta_c = \frac{K\lambda E}{\pi\sigma_i s^2}\{1 - e^{-2s}(1 + 2s + 2s^2)\} \tag{1.8}$$

Where U_c is vibratory energy density. Equation 1.8 shows that loss factor does not depend on the vibration frequency.

CHAPTER 2 : LITERATURE REVIEW

B. J. Lazan [10] explained in his work that why study of vibrations near resonance is important, and why damping is needed to control these vibrations. He classified different types of vibration damping, but his main focus was on structural and hysteretic damping. He also investigated different factors which affect the damping characteristics and how these methods can be improved. He developed analytical techniques and proposed design optimizations to improve shear damping for interface adhesive.

D. Kroisová [11] in his work investigated the damping characteristics of a specific type of composite material known as particulate-epoxy composites. These composite materials can be used as passive dampers. He investigated the effect of reinforcement by silicon dioxide and lead on the damping properties (i.e. damping capacity). He also investigated the effect of volume fraction of these reinforcements. He used photoelectric technique for deflection measurement.

C. Hirunyapruk, B.R. Mace and M.J. Brennan [12] in their work, developed an adjustable damper known as Magneto-Rheological Fluid damper. Sometimes the natural frequency changes, and drifts from the excitation frequency of adaptive tuned vibration absorber, and AVTA has to be retuned, so that its excitation and natural frequencies coincide. They solved this problem by adjusting the stiffness. They proposed a three layer AVTA, in which central layer consists of Magneto-Rheological (MR) fluid. This fluid changes its shear stiffness as the applied magnetic field is changed. They used a control system to control the magnetic field and hence the shear stiffness.

Ion Pelinescu and Andrew Christie [13] investigated the damping characteristics of Liquid Applied Structural Dampers (LASD), which is a new special type of coating. They used these coatings to reduce the vibration and noise in automobiles. As modern automobile structures are lighter in weight, and require more sophisticated techniques of damping rather than the old conventional methods. This was the main motivation for their work on automobiles. They performed a number of experiments, initially on beams, and then they extended their work to real automobile structures. Their results show a significant increase in damping loss factor after application of LASD coatings.

F. Ghezzo and X. Miao [14] worked to improve the damping properties of structures under impulsive or shock loadings. They used a composite coating of polyurea to reduce

vibrations, as this coating greatly improves the damping properties of the structures after its application. They also improved the coating material by changing its structure, by reinforcing the coating material with addition of ceramic particles and fibers. They performed their experiments after applying pure polyurea and reinforced polyurea coatings on steel plates, and then measured the damping properties, their results show that plates with reinforced polyurea exhibited better damping properties as compared to pure polyurea coated plates.

Peter [15] used loss modulus as a damping property to compare the damping characteristics of different hard coatings on gas turbine blades. His results show that ceramics coatings have a strong dependence on amplitude of the vibrations, but they are not dependent on temperature or excitation frequency. His results indicate that metallic, bimetallic and metallic-ceramic coatings shows significant damping when applied as thin coating layer as compared to ceramics, and have potential to be used in vibration suppression applications. He also compared the damping properties of air plasma sprays and electron beam vapor deposition coatings, his results indicate that APS shows a damping maximum, while EBPVD doesn't show any such peak.

Cochardt [7] proposed the domain theory, which describes that enhancement in damping in magneto-mechanical materials is through the internal friction caused by stress induced irreversible rotation of domain walls. Smith Birchak [8] improved the work of [7], they showed that the magnetomechanical damping is caused by stress driven irreversible rotation of magnetic domain boundaries. They linked the critical stress with the average internal stress opposing the domain boundary movement. They further extended this work in [9] and included the effects of magnetic field and applied stresses, and improved the accuracy of internal stress distribution function.

Shen [16] performed experiment analysis on compressor and turbine blades and successfully confirmed the damping characteristics of magnetomechanical material coatings, both at room and high temperatures. He used two types of iron chromium based magnetomechanical coatings, Fe-Cr-Mo and Fe-Cr-Al. These coatings were applied by vapor deposition and air plasma spray techniques. He performed his experiments by producing vibratory stresses using dynamic shakers in blades and beams. While he used concentrated harmonic loads for his numerical analysis. His results show significant enhancement in damping parameters and decrease in vibratory stresses of coated blades as compared to uncoated blades.

S. Hussian [17] investigated the damping characteristics of nickel based magneto-mechanical coating on cantilever steel beams by comparing vibration response of coated and uncoated beams, their results show significant improvement in vibration damping of the beams.

Hsin-Yi Yen and M.S [18] worked to improve the durability and integrity of turbine blades. He observed that main reason of turbine blade failures is vibratory stress caused by aerodynamic loadings. These stresses can be reduced to an acceptable level by adding additional dampers or by increasing internal damping. He used Fe-Cr magneto-mechanical coating to improve the damping in turbine blades. In their experiments, they first used cantilever beam samples and determined their damping properties and vibratory stresses under loading. Then they applied magneto-mechanical coatings on these beams, and measured the damping properties and vibratory stresses of coated beams. Their results show a substantial enhancement in damping characteristics, and decrease in vibratory stresses in coated beams as compared to uncoated beams. They also performed FEM analysis, and then extended their FEM model for turbine blades.

I. Aziz et al. [19] used numerically calculated aerodynamic loads on 1.5 stage axial turbine instead of concentrated structured loads to bring more reality to the problem. They applied these loads on coated and uncoated blades through a FEA package. Then they performed forced response analysis at natural frequencies to find vibratory stresses. Their results show significant reduction in vibratory stresses between uncoated and coated blades.

S.H Raza [20] investigated the change in damping of cantilever beams under different magneto-mechanical coating thicknesses by using FEM analysis, their results showed that the damping increases by increasing coating thickness, but after a certain limit, the change in damping is very negligible and further increase in thickness of coatings doesn’t produce any substantial improvement in reduction of vibratory stresses. They also developed an empirical relationship to find optimal thickness of coating.

N. Good, J. Dooley and B. Fultz [21] investigated the damping properties of ferromagnetic polycrystalline TbDy alloys. They used these alloys because they possess very high magnetostriction. Which means a large amount of energy is required to reorient their magnetic domain walls. This energy comes from the vibration energy, which leads to damping of the system. They used different composition of polycrystalline TbDy alloys as samples. The samples were in the form of cylindrical ingots. Then they measured the energy dissipation

caused by vibratory stresses by using hysteresis loop method. Their result show that 99.7% pure polycrystalline Tb76 Dy24 alloy exhibits the best damping/energy dissipation.

K.B. Hathaway [22] investigated the giant magnetostriction alloy Terfenol-D for its magnetomechanical damping properties. They showed that for maximum damping at low amplitude stresses, materials should be selected with larger magnetostriction and small magneto-crystalline anisotropy. While for high amplitude stresses, the largest damping capacities will occur in materials selected with larger magnetic anisotropies. Their results showed that by changing the material microstructure, the damping through purely elastic and eddy current mechanisms can be increased.

D. W. Shoon and his colleagues [23] investigated the effect of changing the microstructure of a magnetomechanical alloy Fe-Al-Mn on its damping characteristics. They tried to find out the microstructure of Fe-6Al-25/34Mn alloys having the best damping characteristics. For this purpose they conducted various experiments on different microstructures. Their results show that the damping capacity increases with the degree of cold work, and it also depends on the volume fraction of ε martensite while it does not depend much on other phases i.e. α' and austenite (γ).

Fuxing Yin and his colleagues [24] investigated the effect of nickel addition on damping properties of Mn-Cu alloys. They used three beams of alloys Mn30, Mn4Ni and Mn6Ni for their experiments. Then they excited these beams at different frequencies. The response of these frequencies was measured and damping capacity was calculated by this response. The maximum damping capacity was observed in Mn6Ni, which means that damping characteristics of Mn-Cu alloys can be increased by addition of Nickel.

A. Karimi [25] found that Al (0-8%) and Mo (0-4%) addition is very beneficial in enhancing the damping capacity due to their smaller magnetic domain sizes, or smaller coercive forces present in these elements. Their results show an optimal chemical composition of 2-4% Al for Fe16%Cr-Al alloy. They also found that annealing the samples up to 1100°C greatly increases the damping capacity, because annealing decreases the internal stresses and increases the magnetostriction constant.

V. F. Coronal [26] investigated the magnetomechanical damping in iron ingots, their results show that the magneto-mechanical damping is dependent on strain amplitude. The

damping increases with increase in strain amplitude till its maximum value, but further increase in strain decreases the damping.

Xili Lu and his colleagues [27] investigated the effect of Cerium addition on damping characteristics of Cu-Al-Mn alloys. They used two different Cu-Al-Mn alloys in their experiments. They used cantilever beams made from these alloys, and measured their damping characteristics with different compositions. Their results show that the addition of Cerium refines the alloy grains, and improves the ductility and strength of the alloys. The damping capacity increases initially with the addition of Ce, and after reaching a maximum level, it decreases. They observed that the composition of (Cu83Al12Mn5) 99.95Ce0.05 has the best damping characteristics among these alloys.

Renrong Lin and his colleagues [28] investigated the effect of Mn and Mo addition on the damping capacity of Fe-Cr-Al alloys. They used three beams with different material compositions, and measured the damping capacity of these alloys. Their results show that Fe-12Cr-1Mn-6Al has the better damping capacity then other two alloys, which means that addition of Mn is beneficial for damping while addition of Mo has little or no effect on the damping properties.

A. Karimi and colleagues [29] investigated the magnetomechanical damping in the plasma sprayed Fe-Cr based coatings, they used Fe-16%Cr-2%Al & Fe-16%Cr coatings on austenitic steel cantilever beams, the damping was measured for frequency range of 10Hz to 10KHz and a strain range of 10^{-3} to 10^{-4}. Their results show that damping capacity is dependent on strain amplitude, it increases to a maximum with increase in strain amplitude, and then it decreases to its initial values if strain amplitude is further increased. They also investigated the effect of excitation frequency on the damping capacity, and their results show that applied frequency does not affect the damping capacity significantly. They also investigated the impact of annealing on the vibration characteristics of the samples, their results show that annealing improves the damping capacity due to enhanced movement of domain walls and the creation of 90^{o} domains.

R. C. Frank [30] investigated the magneto-mechanical damping in Iron-Silicon alloys, they experimented on iron-4% silicon wires with preferred orientation with direction of axis, their results showed even at low strain levels, there was extremely high magnetomechanical damping in a torsion pendulum. They also investigated the effect of static stress on damping, and

the results show that as the internal stress increases, the damping maximum moves to a higher strain values.

J. T. A. Roberts [31] investigated the magneto-mechanical damping of pure nickel and 20% Copper-Nickel alloy.

B. A. Potekhin [32] investigated the effects of annealing on the damping characteristics of Ni and Cu based magnetomechanical coatings deposited on the structural steel, their results show that annealing increases the damping properties substantially. Annealing the specimens to 1000°C for 2h completely recrystallizes the Ni and Cu coatings and enhances their deformability, which increases damping in these coatings. Their experiments also revealed that carburization of coating thickness significantly reduces the damping capacity.

CHAPTER 3 : EFFECT OF MAGNETOMECHANICAL COATING ON BEAMS OF DIFFERENT SIZES

3.1 Experimental Work

3.1.1 Objective:

The objective of this work is to study the effect of 200μm magnetomechanical coating on beams of different thicknesses (2-3mm) on their damping properties. For this purpose mild steel beams were manufactured, and were mounted in cantilever position. Then their natural frequencies were determined using bump test. And their maximum displacements were determined by forced response at first natural frequencies. The damping ratios were found using logarithmic decrement method by comparing amplitude of peaks using time domain settings on vibration analyzer. Then the beams were coated with a Nickel-Aluminum based magneto-mechanical coating of 200μm thickness using plasma arc method. After the coating, the experiments were repeated for coated beams, so that results can be compared with uncoated beams.

3.1.2 Beams

In accordance with ASTM standard E-576-93, Mild steel beams were machined having dimension 180mm x 10mm x t. Where t represents the thickness. There were 7 beams manufactured having thicknesses of 2, 2.1, 2.2, 2.3, 2.4, 2.5 and 3mm. The beams are shown in figure 3-1. And their physical properties are given in table 3-1.

Table 3-1: Beam Properties

Material	**Mild Steel (MS)**
Dimensions	180mm x 10mm x t
Young's Modulus	2×10^{11} Pa
Poison's Ratio	0.3
Density	7850 Kg/m^3

Figure 3-1: Beams manufactured for experimental analysis

3.1.3 Coating

The magnetomechanical coating of Ni_3Al is used in this work, the chemical composition of the coating is given in table 3-2

Table 3-2: Chemical Composition of Coating

Coating	**Nickel based Alloy**
Nickel (Ni)	80 %
Aluminum (Al)	20 %
Cobalt (Co)	0.5%

While the physical properties are given in table 3-3

Table 3-3: Coating Material Properties

Material	Ni_3Al
Young's Modulus	2.04×10^{11} Pa
Poison's Ratio	0.315
Density	6900 Kg/m^3

3.1.3.1 Coating Technique

Plasma arc method was used to apply the coating on beams. The beams were chemically cleaned, and then were sand blasted for proper adhesion on the surface, and to avoid chipping off due to vibrations. In this work, coating thickness of 200µm was attained.

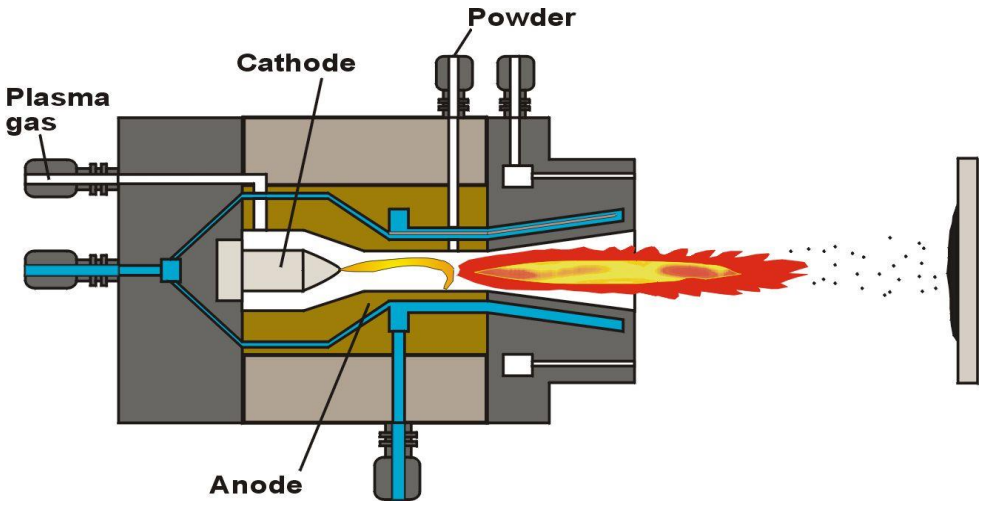

Figure 3-2: Plasma Arc Coating method

3.1.4 Natural Frequencies

To find the natural frequencies of the beams, bump tests were conducted. In this method, the beams are clamped from one end and an accelerometer is mounted on the free end of the beam as shown in figure 3-3. The beams are then excited by hitting the beams near the free end of the beam. As the beams vibrate freely, they vibrate at their natural frequencies, which are then determined using the vibration analyzer. Only first 3 bending mode frequencies are determined in this work.

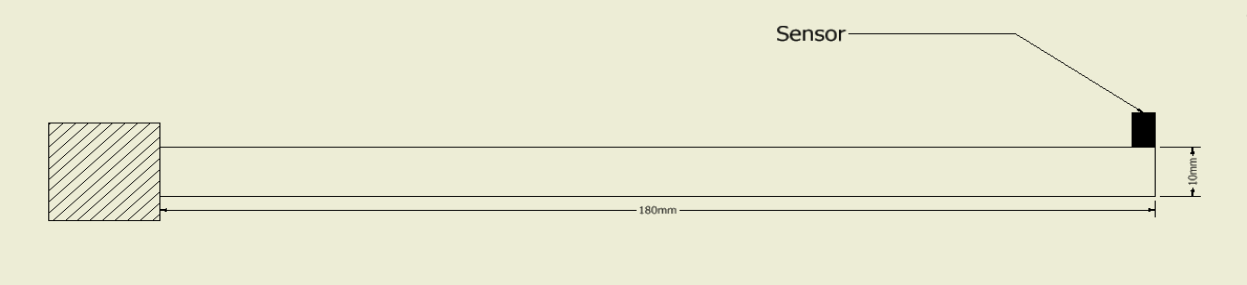

Figure 3-3: Experimental setup for hammer tests

3.1.4.1 Instruments used

Brüel & Kajer sensor shown in figure 3-4, was used as accelerometer in this analysis. The sensor was mounted at the free end of the beams. Sensor settings for the experiments are given in table 3-4.

Table 3-4: Sensor Settings for determination of natural frequency

Sensitivity	1.51pC/g
Maximum frequency	26KHz
Transverse sensitivity	3.8 % of Sensitivity
Maximum continues sinusoidal	5000g peak

Figure 3-4: Accelerometer (B&K-4374)

Sensor's output was connected to a charge amplifier. For these experiments, B&K 2626 amplifier was used, which is shown in figure 3-5. Details of amplifier settings are shown in table 3-5.

Table 3-5: Charge Amplifier Settings for determination of natural frequency

Sensitivity	1.51pC/g
Minimum frequency	1Hz
Maximum frequency	30KHz

Figure 3-5: Charge Amplifier B&K 2626

The charge amplifier output was given to a vibration analyzer. Vibration Analyzer SD 380 was used in these experiments, which is shown in figure 3-6. Before hammer test, following settings are made on analyzer as given in table 3-6.

Table 3-6: Vibration Analyzer settings for determination of natural frequency

Mode of display	Frequency domain
Maximum Frequency	1-2K Hz
Voltage	1V

Figure 3-6: Vibration Analyzer SD 380

3.1.4.2 Experimental Work

After all the above mentioned settings, beams were mounted in cantilever position, and were excited by a hammer as shown in figure 3-7. The frequency upper limit was set to 1KHz–2KHz to obtain natural frequencies. The numerical values of natural frequencies are given in table 3-7.

Figure 3-7: Setup to find Natural Frequencies

Table 3-7: Natural Frequencies of Beams

	1st Natural Frequencies			**2nd Natural Frequencies**			**3rd Natural Frequencies**		
Beam Thickness (mm)	**Uncoated**	**Coated**	**Increase (%)**	**Uncoated**	**Coated**	**Increase (%)**	**Uncoated**	**Coated**	**Increase (%)**
2.0	48.75	53.75	10.3	266.25	307.00	15.3	762.50	881.25	15.6
2.1	52.50	57.50	9.5	296.25	340.00	14.8	843.75	960.00	13.8
2.2	55.00	60.00	9.1	320.00	352.00	10.0	902.49	995.00	10.3
2.3	56.25	61.25	8.9	318.75	343.75	7.8	907.50	972.50	7.2
2.4	60.00	65.00	8.3	342.50	390.00	13.9	971.24	1095.0	12.7
2.5	62.50	67.50	8.0	375.00	395.00	5.3	1052.00	1110.0	5.5
3.0	72.50	77.50	6.9	432.49	465.00	7.5	1215.00	1310.0	7.8

The results show that the coating was most effective in case of thin beams instead of thick beams as it increased the natural frequency of 2mm beam by 10.3% as compared to 6.9% increase in the case of 3mm beam. Comparison of 1st natural frequencies are presented in figure 3-8, percentage changes in 1st natural frequencies is presented in figure 3-9. And the sample graphical results from vibration analyzer for 2mm beam are shown in figure 3-10 and 3-11.

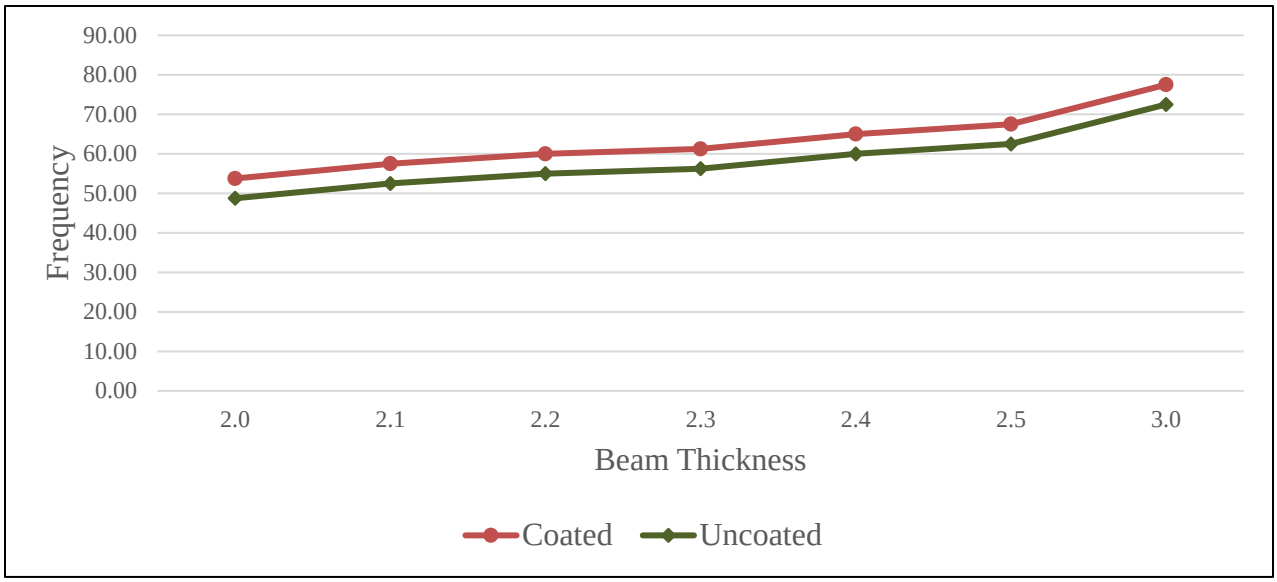

Figure 3-8: Comparison of 1st Natural Frequencies

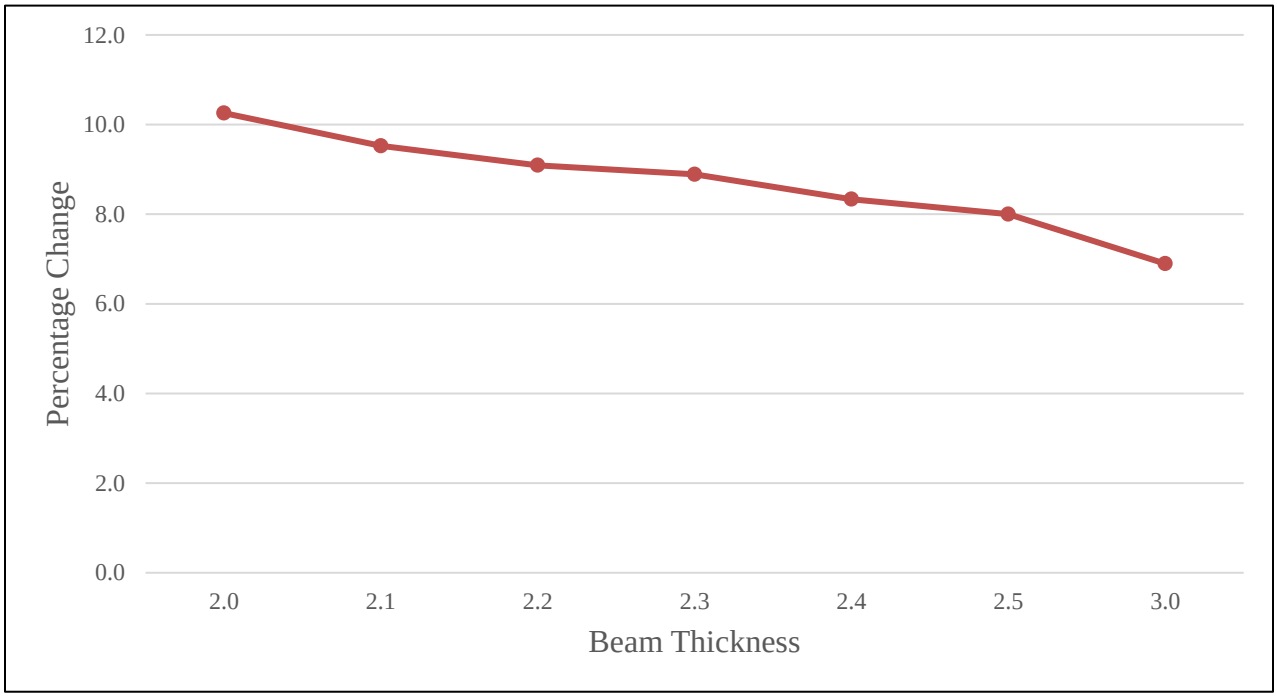

Figure 3-9: Percentage Change in 1st Natural Frequencies

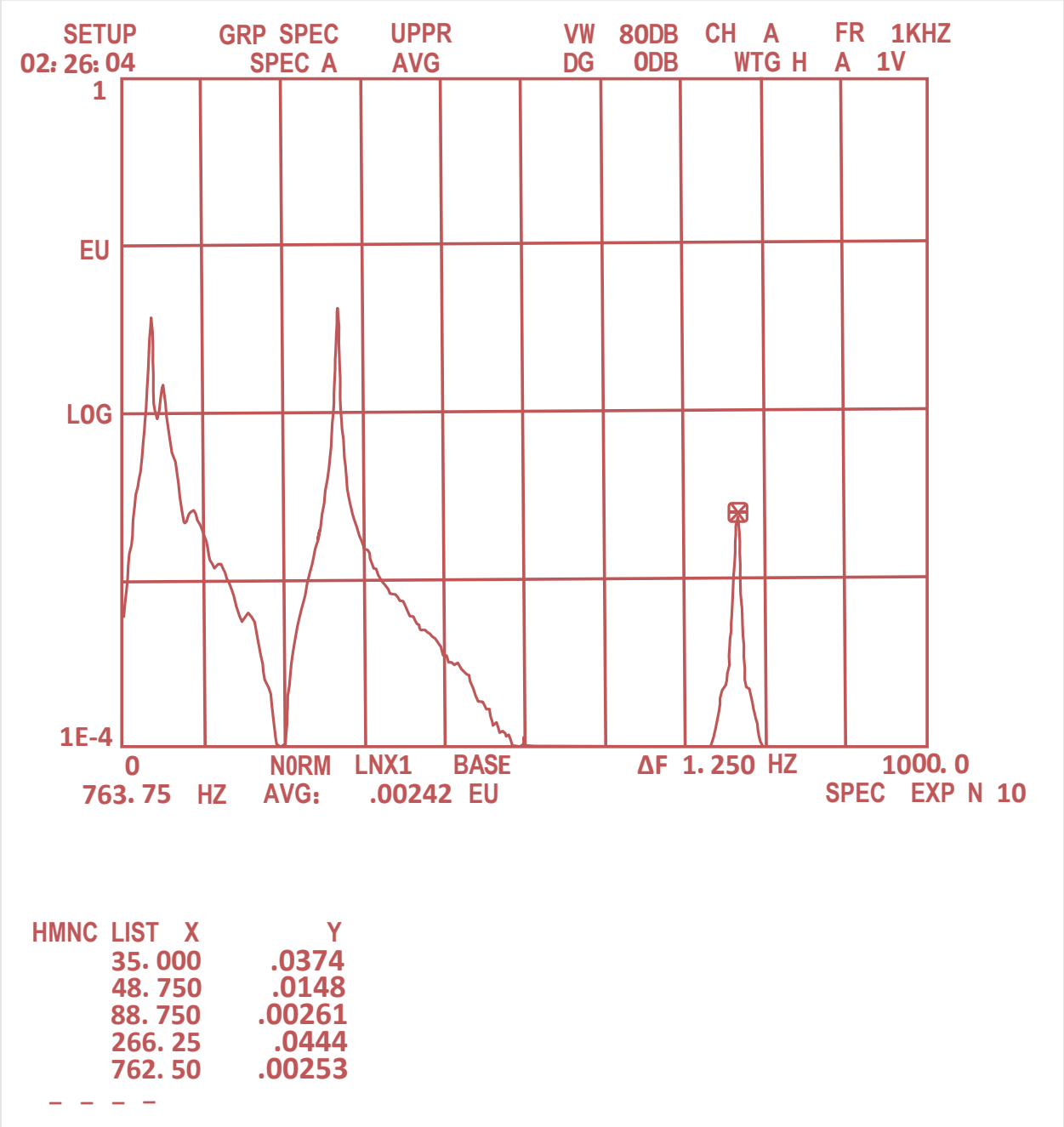

Figure 3-10: Natural Frequencies of 2mm Beam (Uncoated)

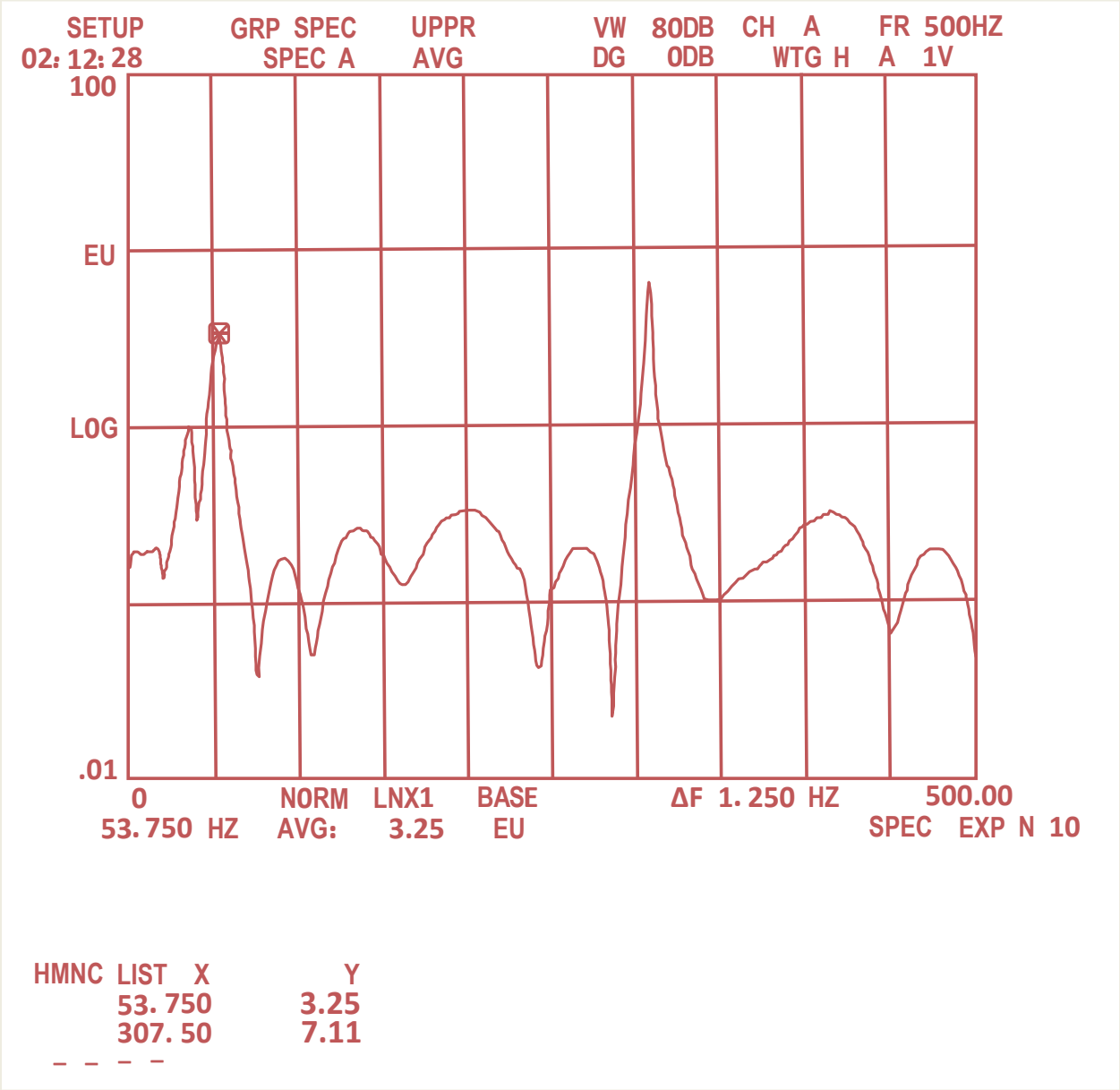

Figure 3-11: Natural Frequencies of 2mm Beam (Coated)

3.1.5 Maximum Displacement

Maximum displacement at the natural frequency of the beams is also a very good measure of the level of vibration under resonance. Therefore, beam's maximum displacements were determined at first natural frequencies.

In this analysis, Brüel & Kajer sensor was used as an accelerometer. The sensor was mounted at the free end of the beams. Sensor settings are shown in table 3-8

Table 3-8: Sensor Settings for determination of maximum displacement

Sensitivity	1.51pC/g
Maximum frequency	26KHz
Transverse sensitivity	3.8% of Sensitivity
Maximum continues sinusoidal	5000g peak

Sensor's output was connected to a charge amplifier. B&K 2626 amplifier was used for this purpose, whose settings are shown in table 3-9.

Table 3-9: Charge Amplifier Settings for determination of maximum displacement

Sensitivity	1.51pC/g
Minimum frequency	1Hz
Maximum frequency	30KHz

The charge amplifier output was given to vibration analyzer. Vibration Analyzer SD 380 was used for this purpose. Following settings are made on analyzer as shown in table 3-10.

Table 3-10: Vibration Analyzer settings for determination of maximum displacement

Mode of display	Frequency domain
Maximum Frequency	1-2K Hz
Voltage	1V

Then the beams were excited by a dynamic shaker through a vibration exciter control, which are shown in figures 3-12 and 3-13, respectively. Details of shaker and vibration exciter control are shown in tables 3-11 and 3-12, respectively.

Table 3-11: Shaker details and settings for determination of maximum displacement

Dynamic Shaker	**B&K 4808**
Power amplifier	2712
current limit	2 A
Amplifier gain	1

Table 3-12: Vibration Exciter Control settings for determination of maximum displacement

Vibration Exciter control	**B&K 1050**
dB level	Auto
Sensitivity	1.51 pC/g
Out put	0-10 V

Figure 3-12: Shaker B&K 4808

Figure 3-13: Vibration Exciter Control B&K 1050

The experiments for maximum displacement measurement were conducted by adjusting the charge amplifier setting on gain-1. The Results of the experiments are given in table 3-13.

Table 3-13: Maximum Displacement of beams at 1st Natural Frequencies

Beam Thickness (mm)	Maximum Displacement (Uncoated Beams)	Maximum Displacements (Coated Beams)	Decrease (%)
2.0	20.7	10.5	49.3
2.1	17.1	9.42	44.9
2.2	13.6	8.64	36.5
2.3	12.2	8.27	32.2
2.4	9.64	6.88	28.6
2.5	8.27	6.18	25.3
3.0	6.37	5.28	17.1

The results of maximum displacement are quite similar to natural frequency results, as maximum percentage change was observed in thin beams (i.e. 2mm beam). Which confirms that the coating was most effective in thin beams as compared to thick beams. Maximum displacements of the beams are plotted in figure 3-14 for both uncoated and coated beams. Percentage changes in beams are plotted in figure 3-15. And graphical results of uncoated and coated 2mm beam are shown in figures 3-16 and 3-17, respectively as samples.

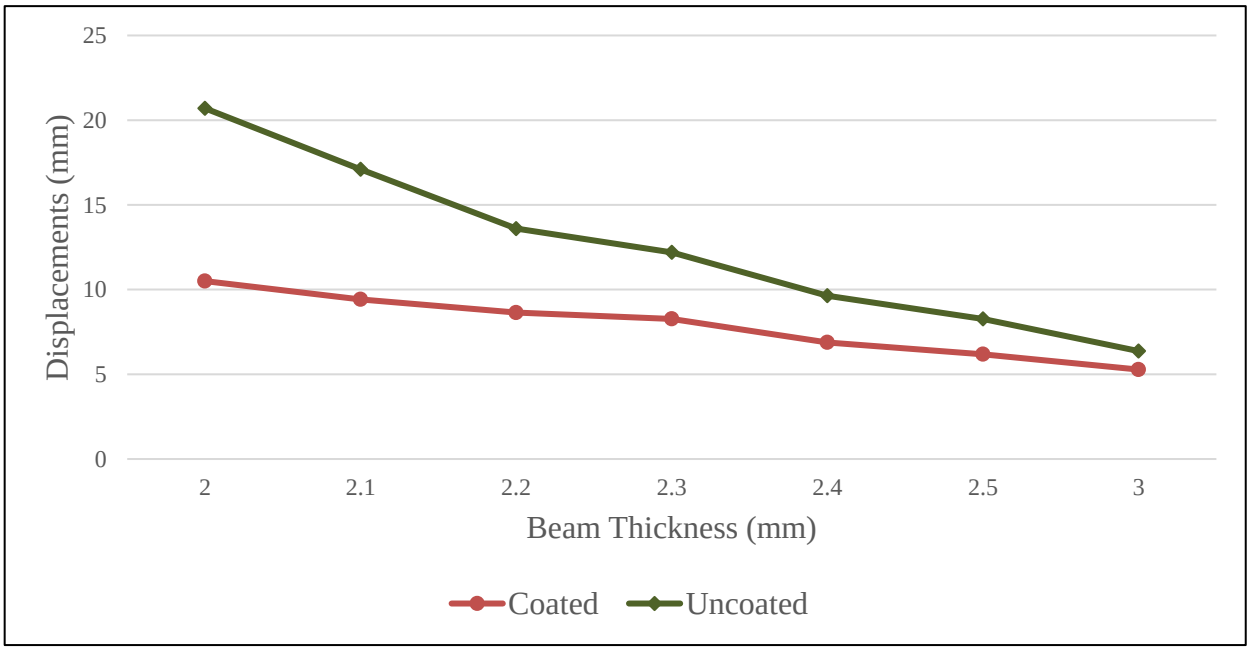

Figure 3-14: Comparison of Maximum Displacements at 1st Natural Frequencies

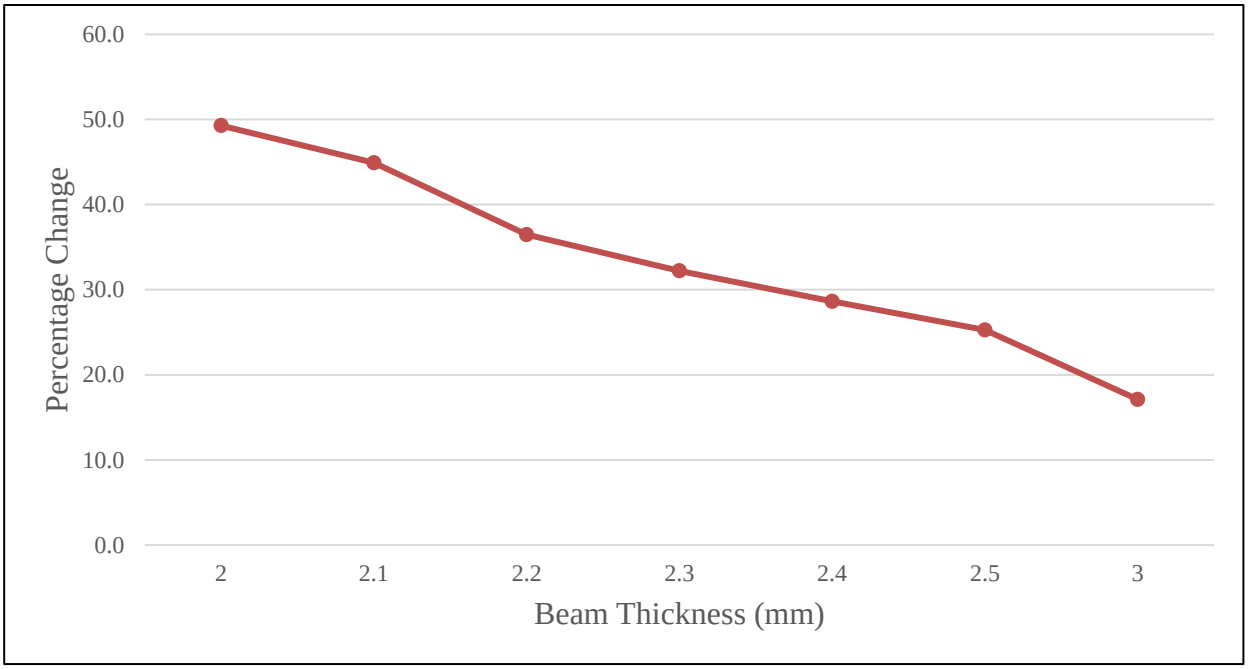

Figure 3-15: Percentage Change in Maximum Displacements

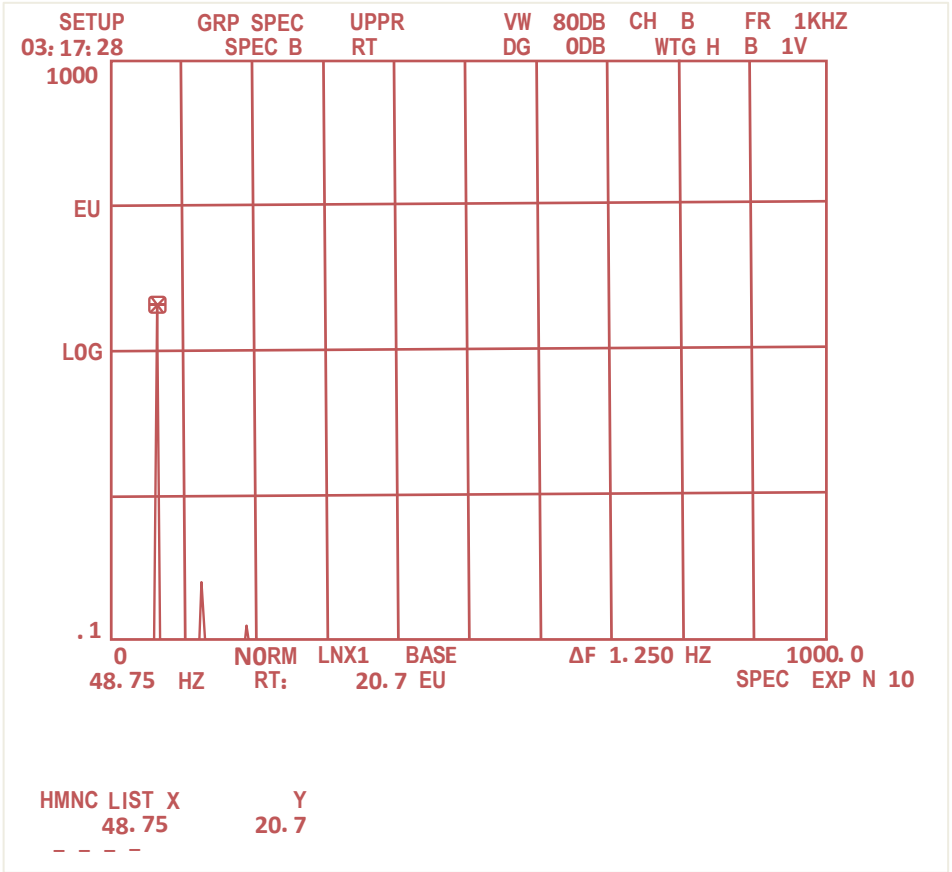

Figure 3-16: Maximum Displacement of 2mm Beam (Uncoated) at 1st natural frequency

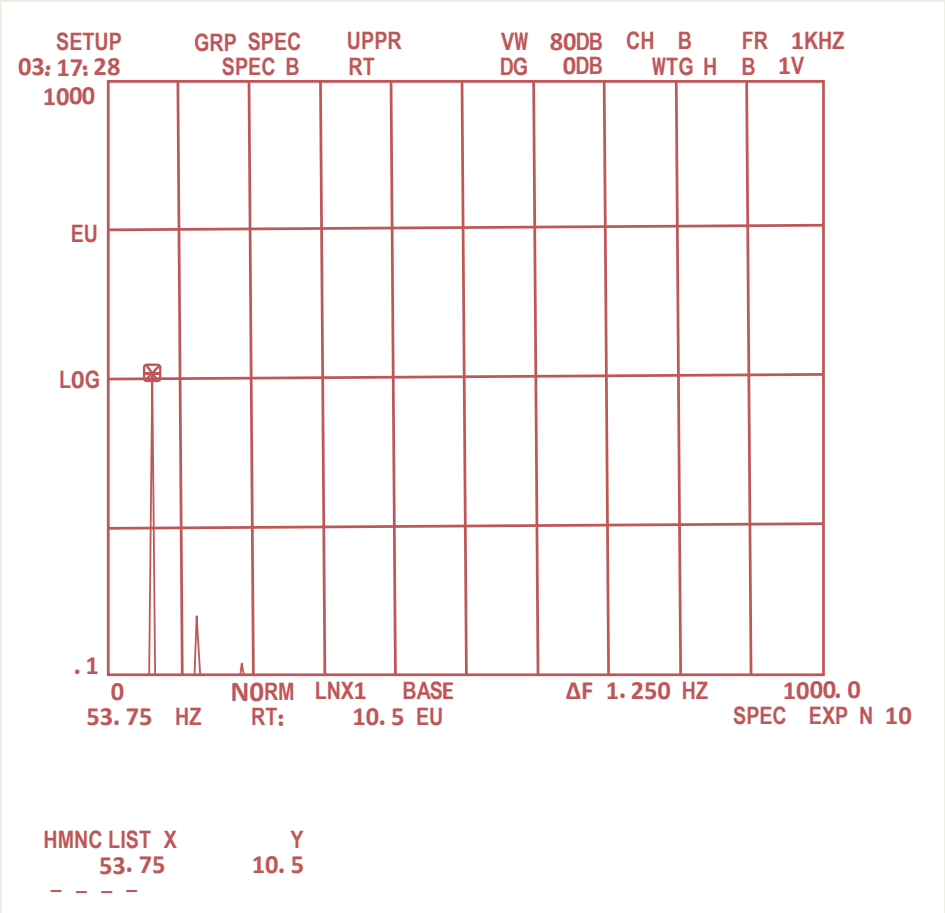

Figure 3-17: Maximum Displacement of 2mm Beam (Coated) at 1st natural frequency

3.1.6 Damping Ratio

Damping ratio is one of the most important parameter to estimate damping in a system. Different methods have been used to determine the damping ratio. In this work, Logarithmic Decrement method was employed. In this technique, the beams are excited by hammer and are allowed to vibrate freely while monitoring their response by adjusting the mode of vibration analyzer in time domain. In this domain the vibration analyzer shows the decay of vibrations over time, the damping ratio is now calculated by logarithmic decrement method.

In this method, first logarithmic decrement is calculated from the equation 3.1

$$\delta = \frac{1}{n} ln \frac{A(t)}{A(t+nT)} \qquad (3.1)$$

Where, A(t+nT) is amplitude of peak n periods away from A(t).

Now damping ratio is calculated by equation 3.2

$$\zeta = \frac{1}{\sqrt{1+\left(\frac{2\pi}{\delta}\right)^2}} \quad (3.2)$$

Configurations of the instruments used for this experiment are shown in tables 3-14 to 3-16.

Table 3-14: Sensor Settings for damping ratio measurement

Sensitivity	1.51pC/g
Maximum frequency	26KHz
Transverse sensitivity	3.8 % of Sensitivity
Maximum continues sinusoidal	5000g peak

Table 3-15: Charge Amplifier Settings for damping ratio measurement

Sensitivity	1.51pC/g
Minimum frequency	1Hz
Maximum frequency	30KHz

Table 3-16: Vibration Analyzer settings for damping ratio measurement

Mode	Time Domain
Frequency	500 Hz
Voltage	0.5V
ΔT	0.781 m Sec

The Damping ratios of uncoated and coated beams for 1st natural frequencies are given in table 3-17.

Table 3-17: Damping Ratios of Beams

Beam Thickness (mm)	**Damping Ratio**		**% Increase**
	Uncoated	**Coated**	
2	0.0097	0.0141	44.8
2.1	0.0109	0.0155	42.5
2.2	0.0122	0.0162	33.3
2.3	0.0128	0.0169	32.4
2.4	0.0142	0.0184	29.1
2.5	0.0154	0.0194	25.9
3	0.0223	0.0256	15.0

The results show a pattern similar to natural frequencies, and the maximum change was observed in 2mm beam (44.8%), while 3mm beam had minimum change in damping after coating (15.0%).

But the percentage changes in damping ratios (15.0-44.8%) are greater than natural frequencies (6.9-10.3%). Which indicates that coating was more effective in reducing damping ratios as compared to its effectiveness to change the natural frequencies of the beams.

Damping ratios of the beams are plotted in figure 3-18 for both uncoated and coated beams. Percentage changes in beam's damping ratios are plotted in figure 3-19. And results of 2mm beam are presented in figures 3-20 and 3-21, respectively as samples.

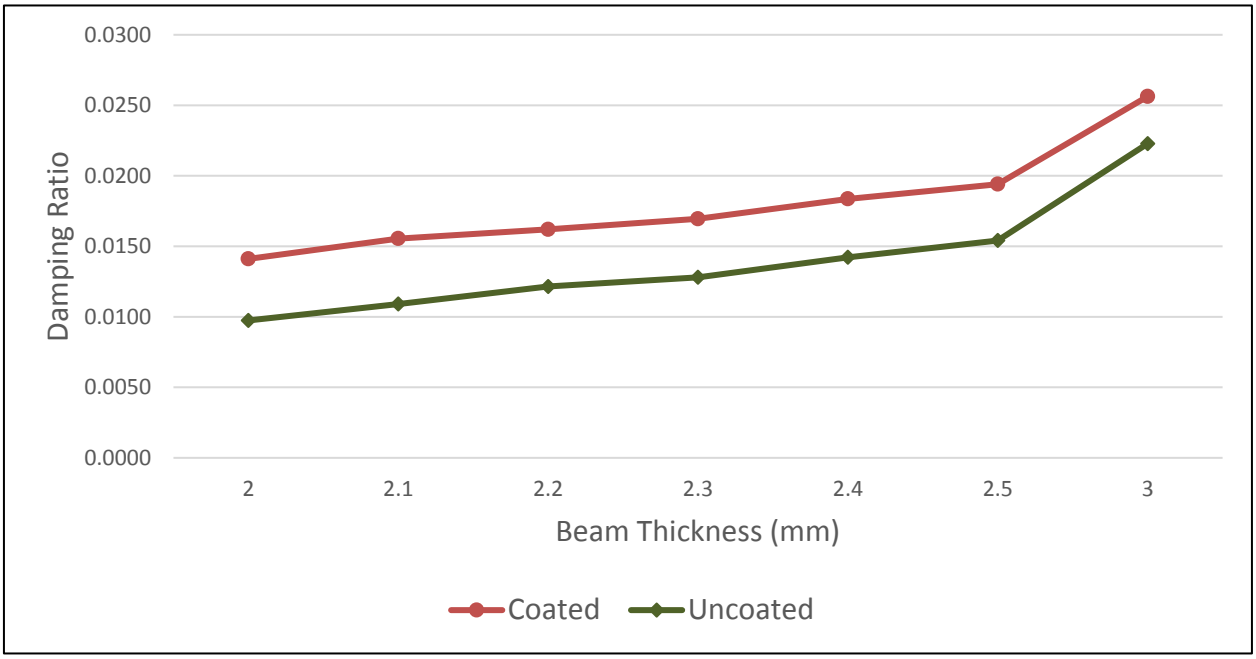

Figure 3-18: Comparison of Damping Ratios

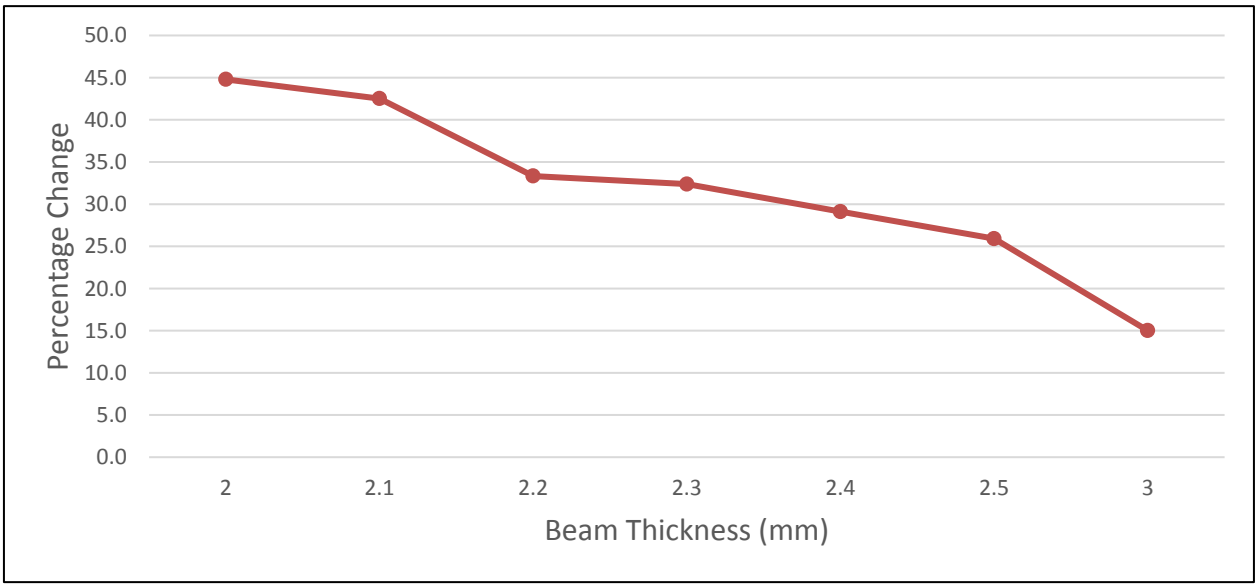

Figure 3-19: Percentage Change in Damping Ratios

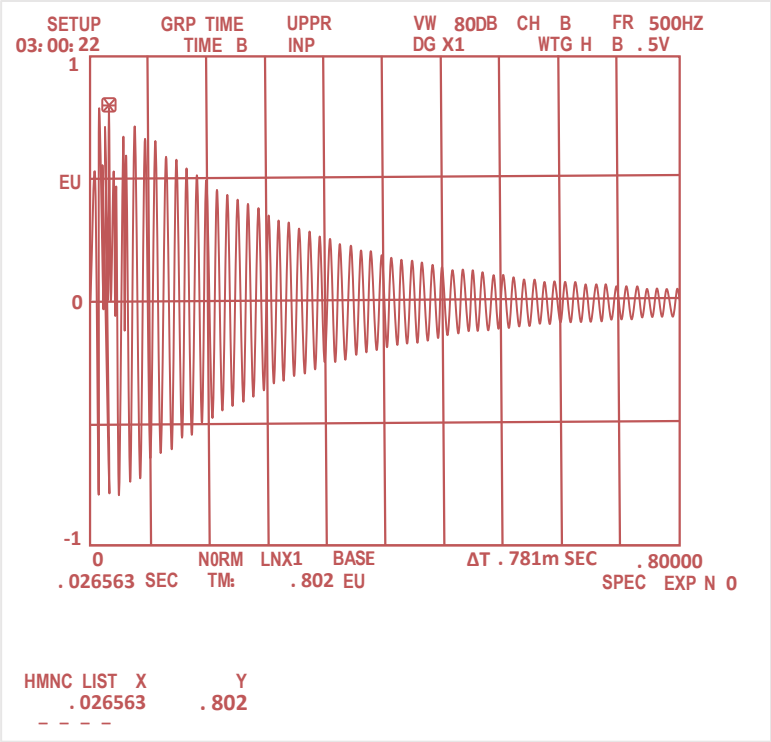

Figure 3-20: Time domain response of 2mm Beam (Uncoated)

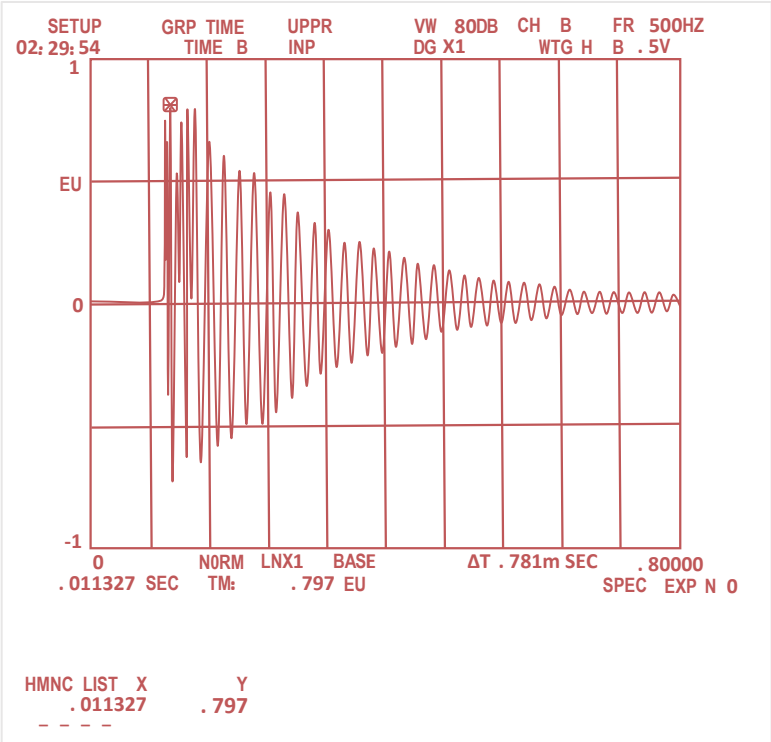

Figure 3-21: Time domain response of 2mm Beam (Coated)

3.2 NUMERICAL ANALYSIS

Numerical analysis is a very valuable tool for modal analysis to find damping properties of a system. Numerical analysis is frequently used to verify the results obtained from actual experiments. And it also helps to design the experimental work, rather than doing it by hit and trial method.

In this work, numerical analysis was performed by using MSC NASTRAN and PATRAN software. First modal analysis was used to find the mode shapes and natural frequencies of uncoated beams. Then harmonic analysis was performed by forced excitation at natural frequencies. The modal and harmonic analysis were again performed after application of coating material to the uncoated beams.

3.2.1 Numerical Analysis Procedure

For the numerical analysis, the beams are modeled in Hypermesh using Psolid elements for beams and PSHELL elements for coating material. 3600 Psolid elements were used to model the beams, and 1800 PSHELL elements were used for modeling of coating material.

Then the geometry was imported into MSC PATRAN, where all the properties and boundary conditions were specified. For this analysis, the beams were fully constrained at one end and a force of 0.1N was applied at the free end of the beams. Then the modal analysis was performed to find the natural frequencies and mode shapes of the beams.

Then harmonic analysis is performed by exciting the beams at their natural frequencies, for harmonic analysis of coated beams, every PSHELL element of the coatings was given separate material properties (i.e. damping ratio) by editing the input file in a text editor. After that several iterations are performed by running analysis and then using stress values of each PSHELL element to recalculate damping factors by using equation 1.8. And using new damping ratio values again in the input file to repeat the analysis until the convergence of the results. Flow chart of the numerical analysis procedure is shown in figure 3-22.

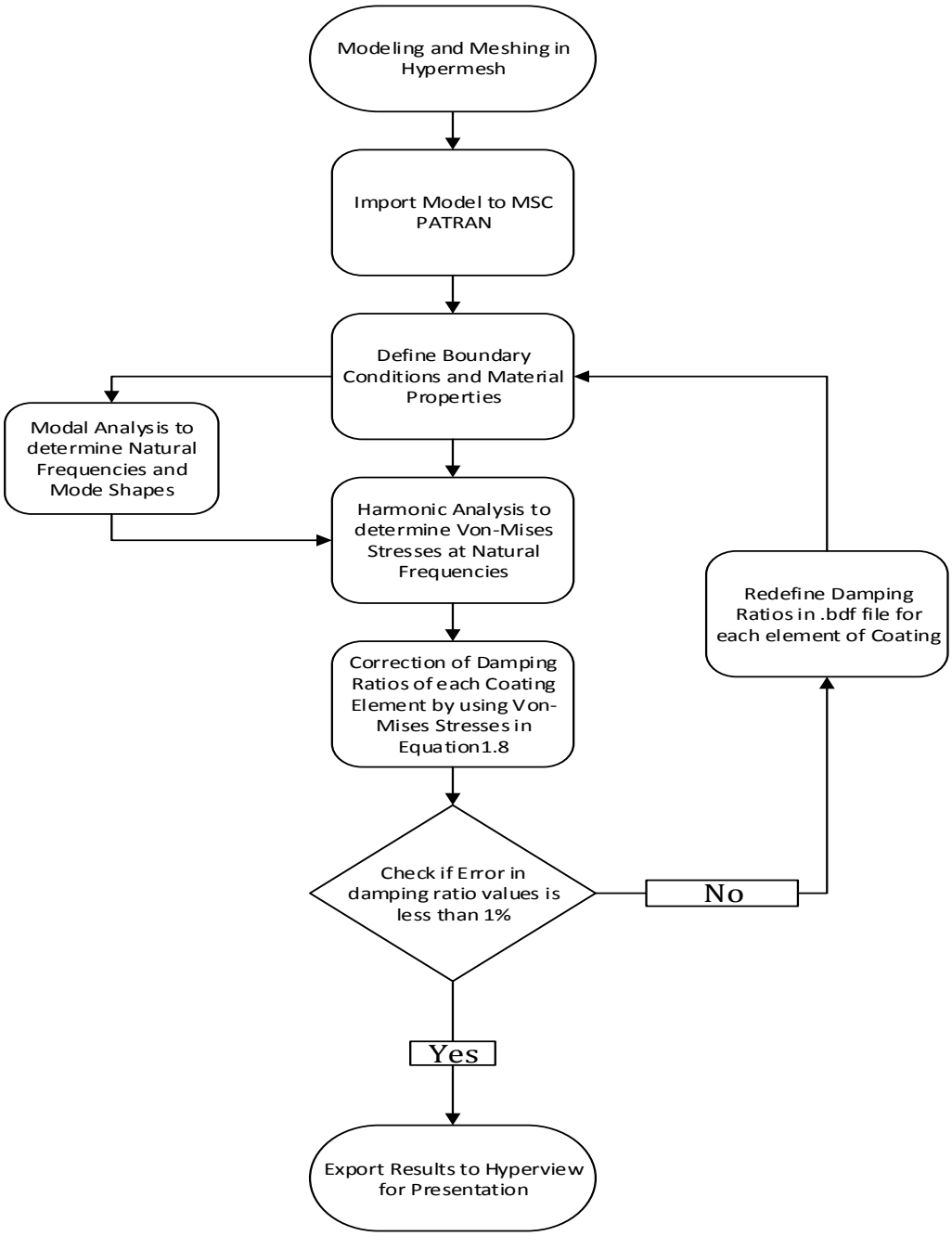

Figure 3-22: Flow Chart of Numerical Analysis Procedure

3.2.2 Modal Analysis

Modal analysis of uncoated and coated beams was performed to find the mode shapes and natural frequencies of uncoated and coated beams.

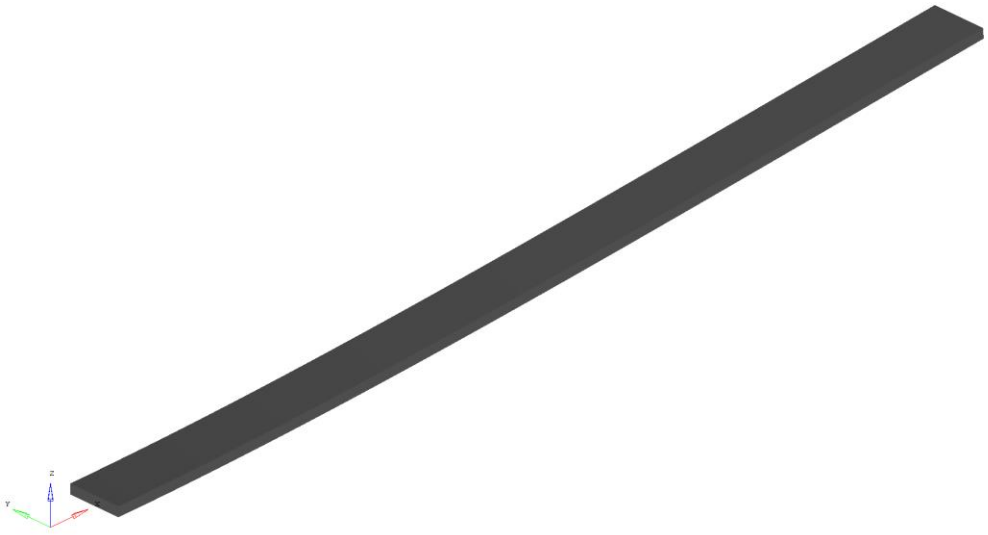

Figure 3-23: Beam for Modal Analysis

3.2.2.1 Natural Frequencies of beams

Natural Frequencies of uncoated and coated beams are shown in table 3-18. Only bending modes are considered in this analysis.

Table 3-18: Natural Frequencies of Uncoated and Coated beams

	1st Natural Frequencies			**2nd Natural Frequencies**			**3rd Natural Frequencies**		
Beam Thickness (mm)	**Uncoated**	**Coated**	**Increase (%)**	**Uncoated**	**Coated**	**Increase (%)**	**Uncoated**	**Coated**	**Increase (%)**
2	49.74	55.22	11.0	311.55	345.78	11.0	871.76	967.32	11.0
2.1	52.52	57.99	10.4	328.90	363.13	10.4	920.22	1015.70	10.4
2.2	55.54	61.02	9.9	347.83	382.05	9.8	973.04	1068.50	9.8
2.3	57.56	63.04	9.5	360.44	394.68	9.5	1008.20	1103.70	9.5
2.4	60.59	66.06	9.0	379.35	413.57	9.0	1061.00	1156.40	9.0
2.5	62.85	68.33	8.7	393.53	427.74	8.7	1100.60	1195.90	8.7
3	74.70	80.17	7.3	467.53	501.70	7.3	1306.70	1401.70	7.3

Results show that the coating of 200µm is most effective when applied to 2mm beam as compared to thicker beams, as it increased the natural frequencies of the beam by 11%, while it increased the natural frequencies of 3mm beam by only 7.3%. It is also observed that all the natural frequencies are increased with same percentage. Graphical plot Comparison of coated and uncoated 1st natural frequencies are presented in figure 3-24. While percentage change in natural frequencies is presented in figure 3-25.

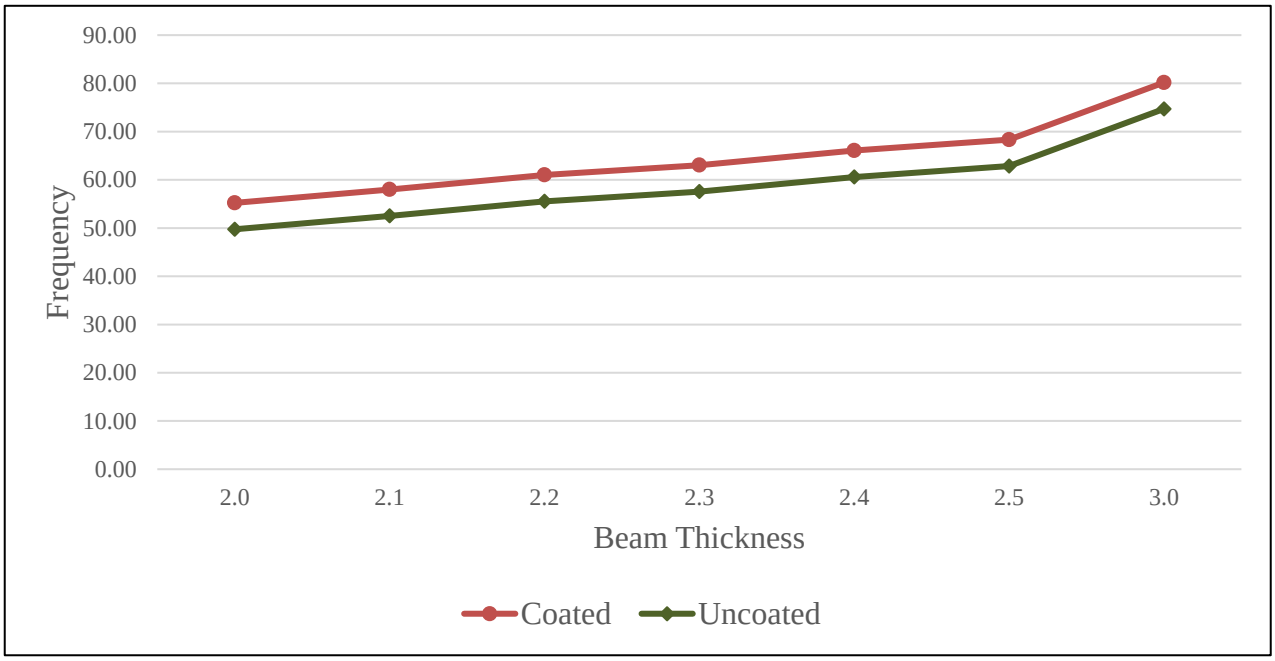

Figure 3-24: Comparison of 1st Natural Frequencies

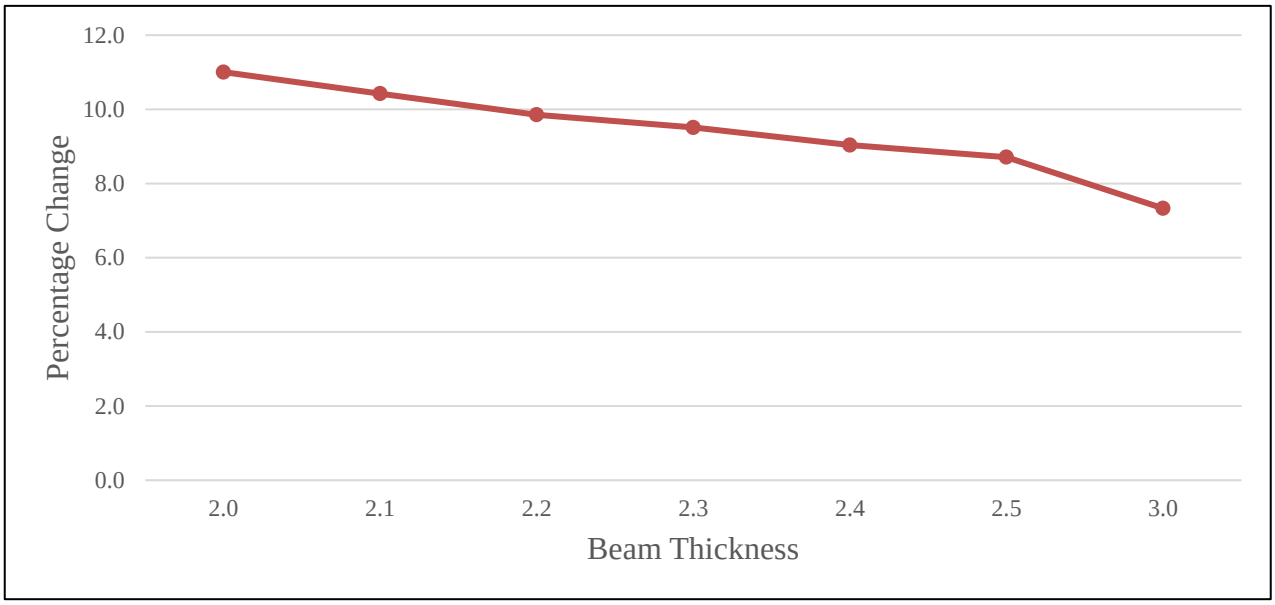

Figure 3-25: Percentage Change in Natural Frequencies

3.2.2.2 Mode Shapes of Uncoated Beams

The 1st, 2nd and 3rd bending Mode shapes of uncoated and coated Beam (2mm) are shown in figures 3-26 to 3-31 as samples, natural frequencies are also indicated in these figures. The mode shapes are almost identical for coated and uncoated beams as the coating was thin as compared to the beam thickness.

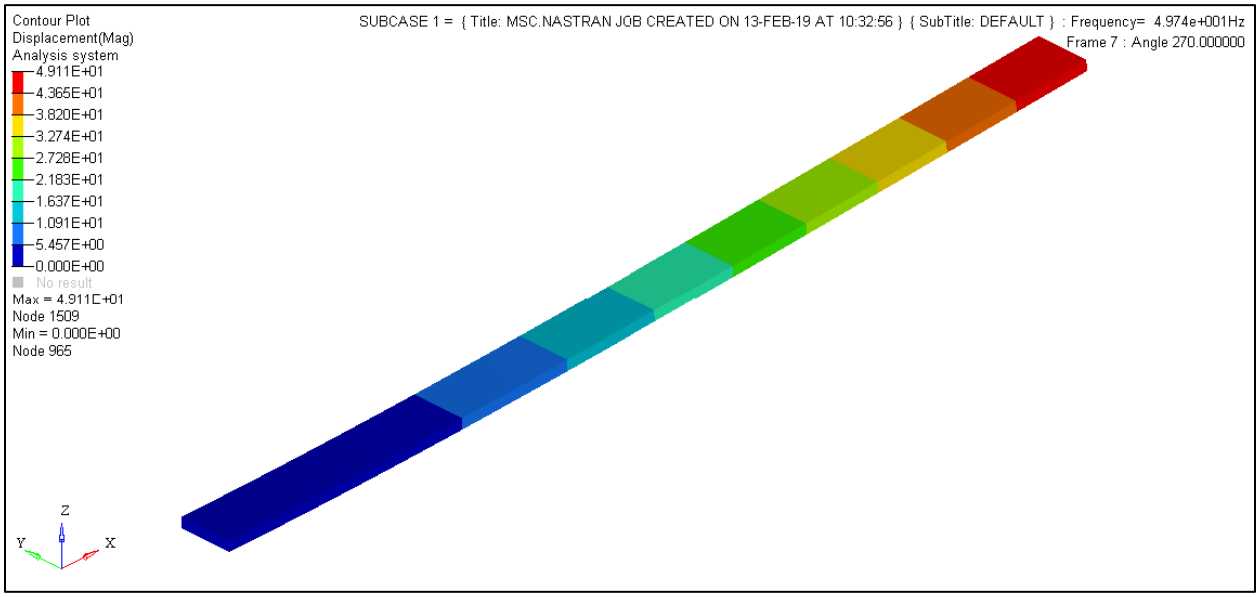

Figure 3-26: 1st Natural Frequency (2mm-Uncoated beam)

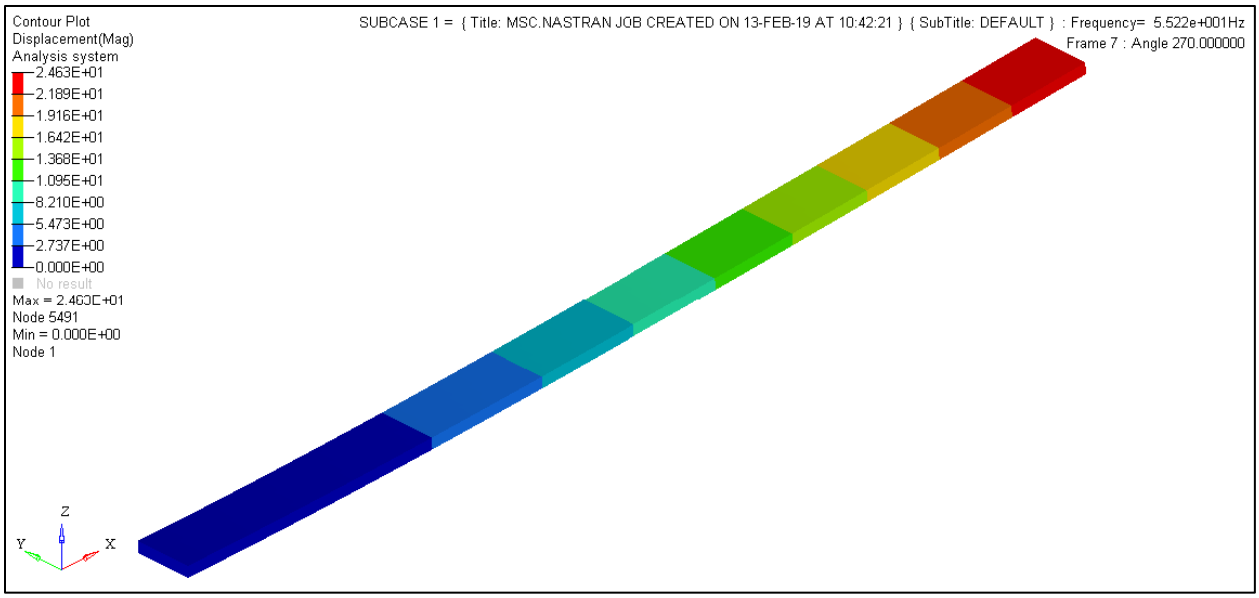

Figure 3-27: 1st Natural Frequency (2mm-Coated beam)

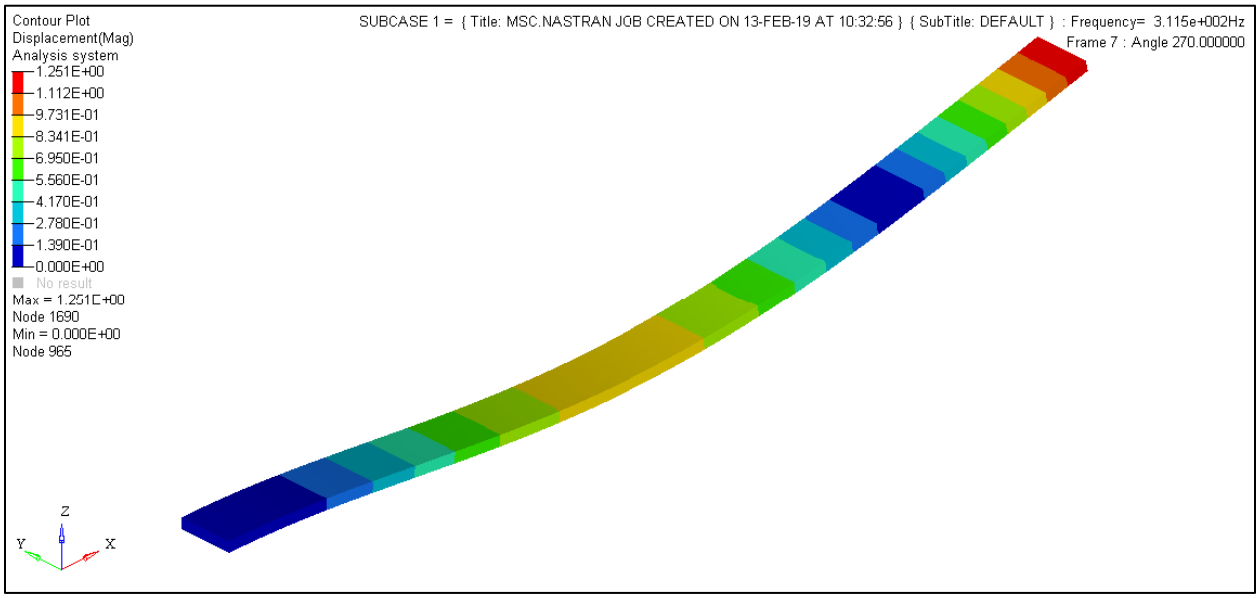

Figure 3-28: 2nd Natural Frequency (2mm-Uncoated beam)

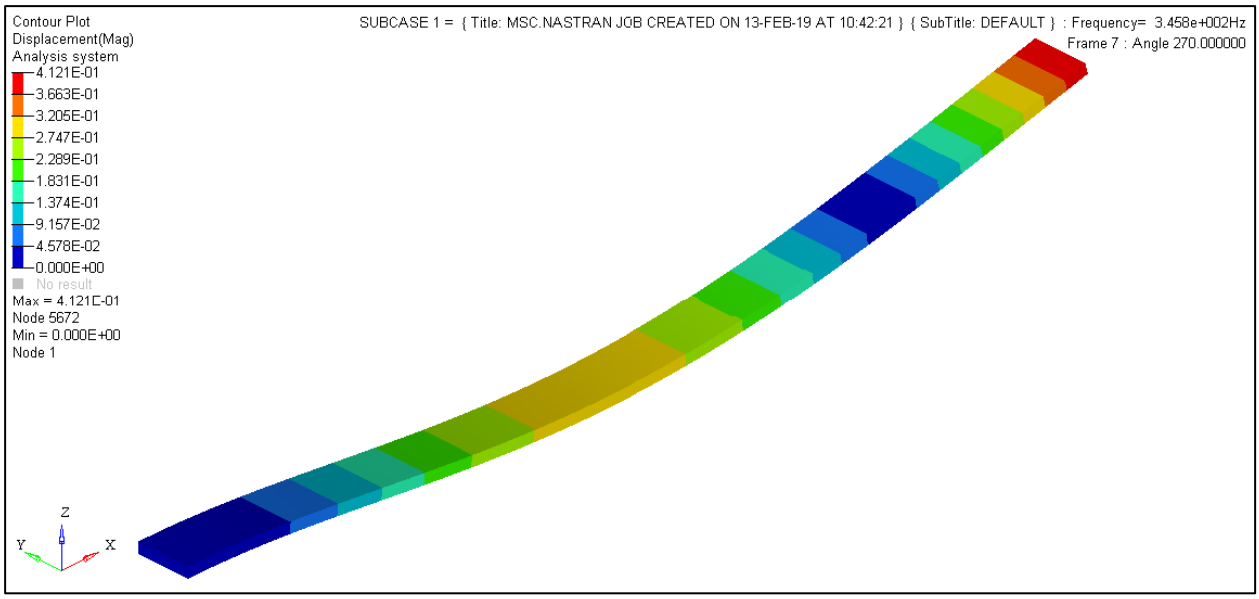

Figure 3-29: 2nd Natural Frequency (2mm-Coated beam)

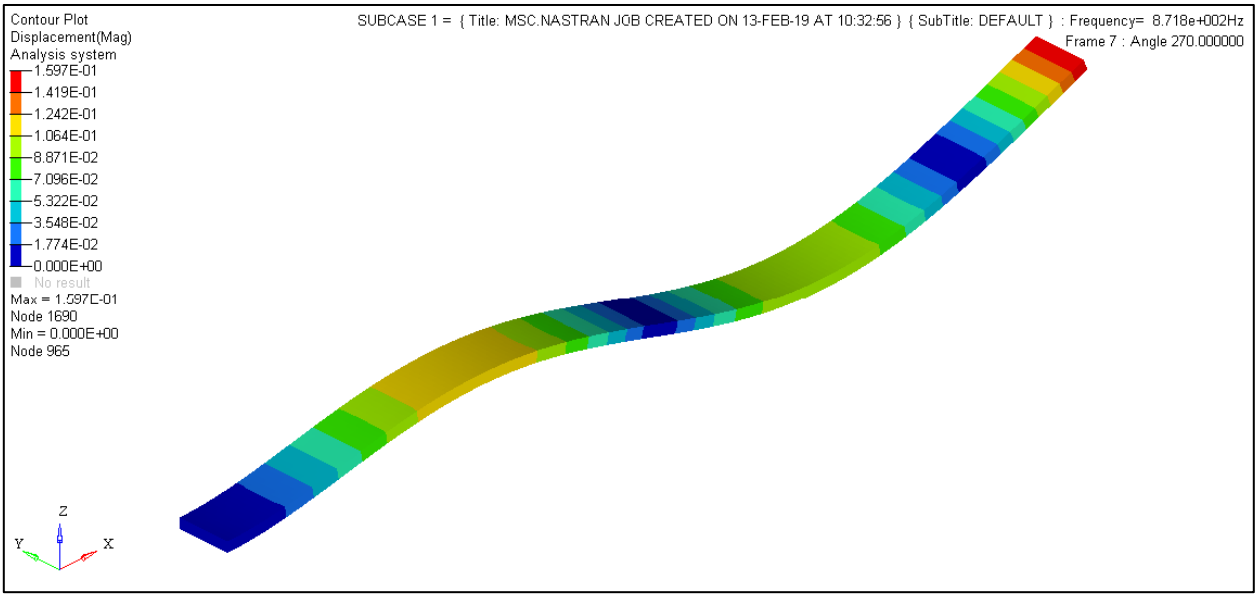

Figure 3-30: 3rd Natural Frequency (2mm-Uncoated beam)

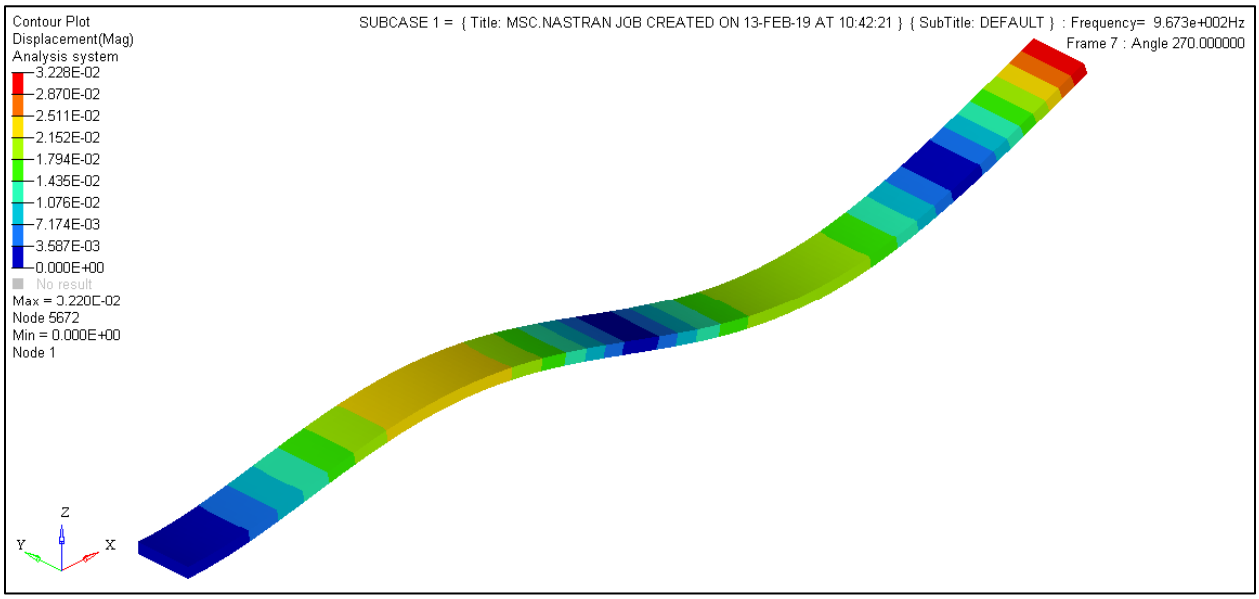

Figure 3-31: 3rd Natural Frequency (2mm-Coated beam)

3.2.3 Harmonic Response

Harmonic response has been obtained by exciting the uncoated and coated beams at 1st and 3rd natural frequencies, the Maximum displacements and Von-Mises stresses of uncoated and coated beams are shown in tables 3-19 to 3-22.

Table 3-19: Von-Mises Stresses at 1st Natural Frequencies

Von-Mises Stresses (MPa)			
Beam Thickness (mm)	**Un-coated**	**Coated**	**% Reduction**
2	1086.00	599.90	44.8
2.1	972.50	576.00	40.8
2.2	867.50	542.20	37.5
2.3	806.50	519.20	35.6
2.4	726.20	488.00	32.8
2.5	673.50	480.20	28.7
3	472.20	386.50	18.1

Table 3-20: Maximum Displacement at 1st Natural Frequency

Maximum Displacement (mm)			
Beam Thickness (mm)	**Un-coated**	**Coated**	**% Reduction**
2	49.11	24.63	49.8
2.1	41.73	22.56	45.9
2.2	35.27	20.24	42.6
2.3	31.69	18.79	40.7
2.4	27.17	16.89	37.8
2.5	24.33	16.10	33.8
3	14.49	11.07	23.6

Table 3-21: Von-Mises Stresses at 3rd Natural Frequencies

Von-Mises Stresses (MPa)			
Beam Thickness (mm)	**Un-coated**	**Coated**	**% Reduction**
2	59.33	4.62	92.2
2.1	53.14	4.48	91.6
2.2	47.41	4.32	90.9
2.3	44.05	4.19	90.5
2.4	39.71	4.07	89.7
2.5	36.80	3.96	89.2
3	25.85	3.55	86.3

Table 3-22: Maximum Displacement at 3rd Natural Frequency

Maximum Displacement (mm)			
Beam Thickness (mm)	**Un-coated**	**Coated**	**% Reduction**
2	0.16	0.0113	92.9
2.1	0.14	0.0105	92.3
2.2	0.11	0.0096	91.6
2.3	0.10	0.0090	91.2
2.4	0.09	0.0084	90.5
2.5	0.08	0.0079	90.0
3	0.05	0.0061	87.2

The Results show that the coating is most effective when applied to thin beams as compared to thicker beams, as it reduced the Von-Mises Stress and Maximum displacement of the 2mm beam by 44.8% and 49.8%, respectively. While it reduced the Von-Mises stress and maximum displacement of the 3mm beam by only 18.1% and 23.6%, respectively for 1st natural frequency. The results also indicate that coatings are more effective at 3rd natural frequencies as

compared to 1st natural frequencies as stresses are reduced by 87-92% in case of 3rd natural frequency as compared to stress reductions of 18-44% in case of 1st natural frequencies.

Graphical Comparison of coated and uncoated Von-Mises Stresses and maximum displacements at 1st and 3rd natural frequencies are presented in figures 3-32 to 3-35.

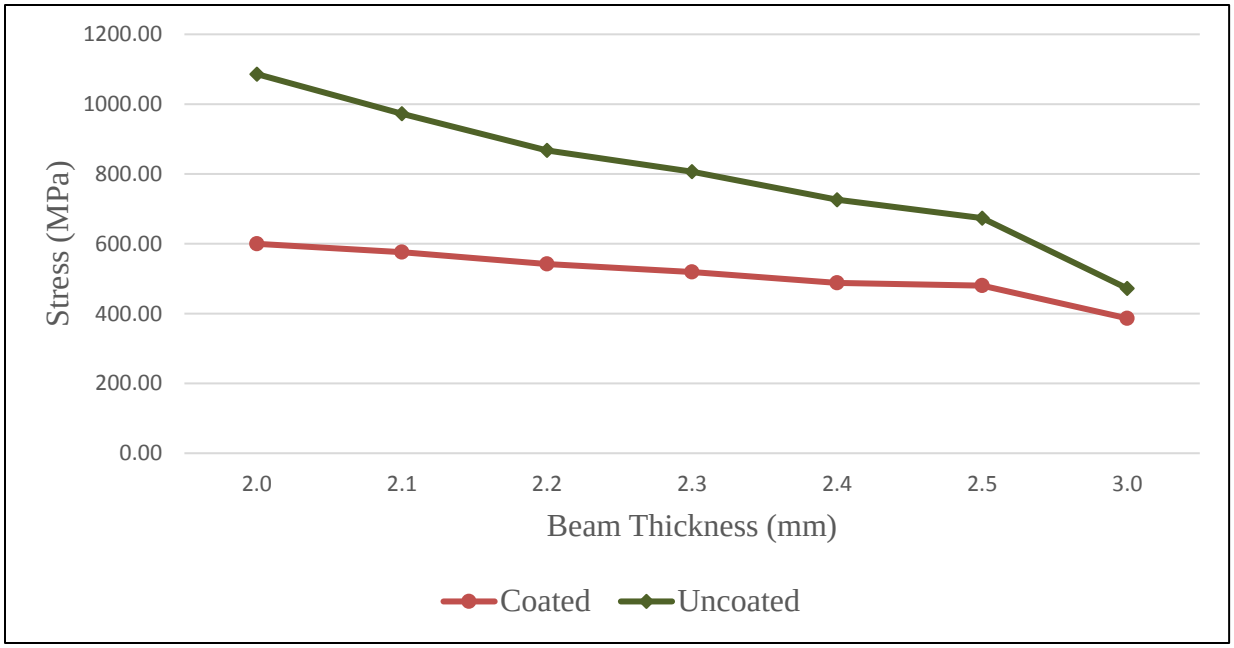

Figure 3-32: Comparison of Von-Mises Stress at 1st Natural Frequencies

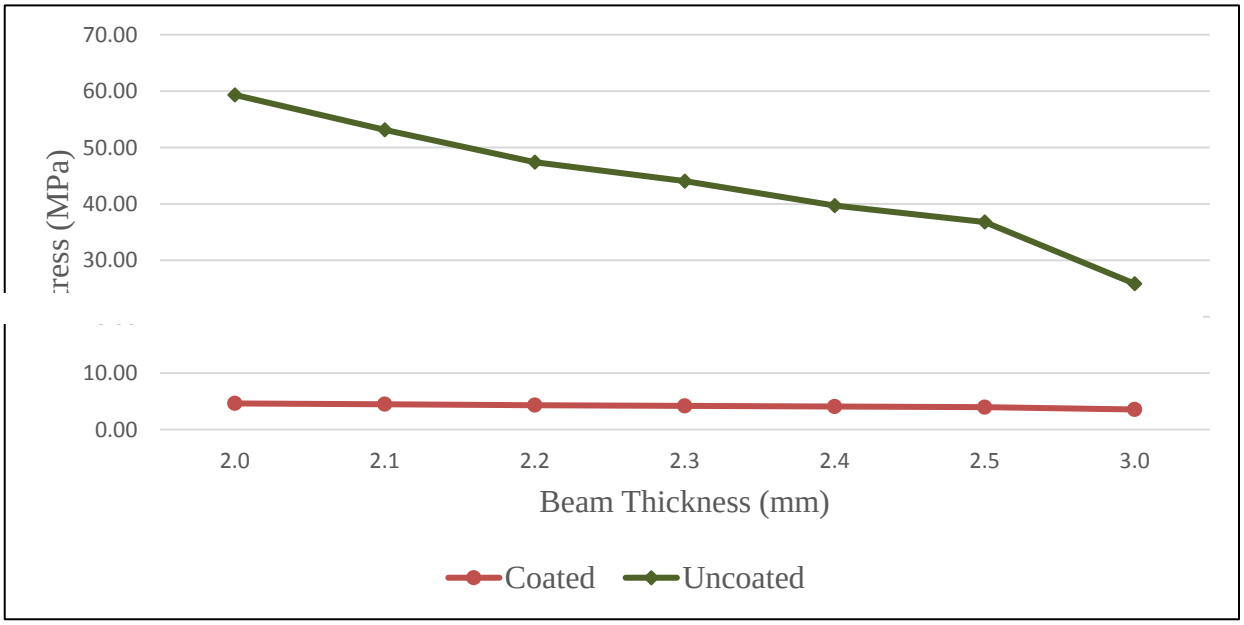

Figure 3-33: Comparison of Von-Mises Stress at 3rd Natural Frequencies

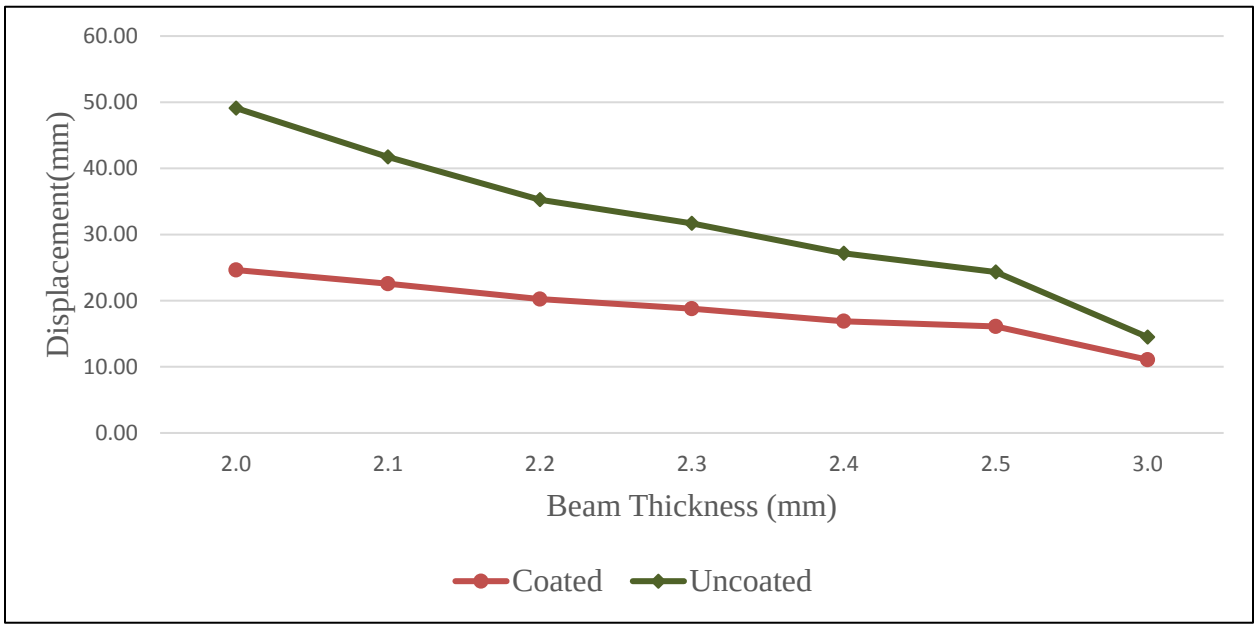

Figure 3-34: Comparison of Maximum Displacement at 1st Natural Frequencies

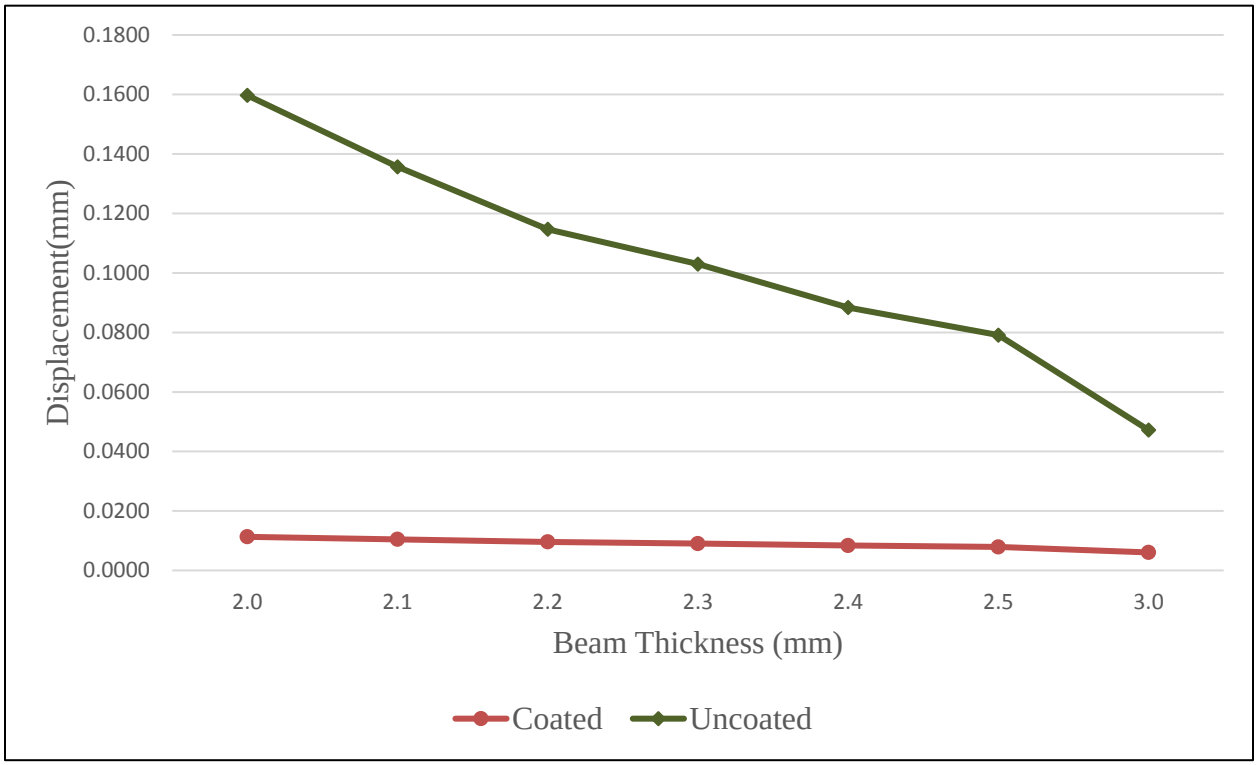

Figure 3-35: Comparison of Maximum Displacement at 3rd Natural Frequencies

Sample contour plots of 2mm beam are presented in figures 3-36 to 3-43.

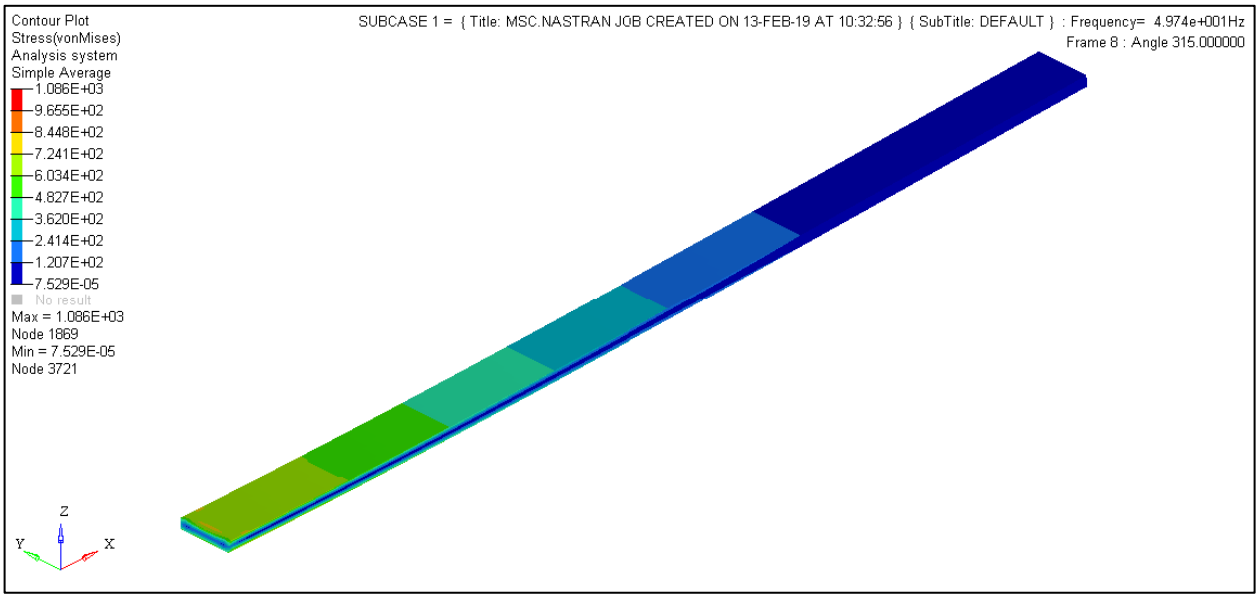

Figure 3-36: Von-Mises Stress at 1st Natural Frequency (Uncoated beam)

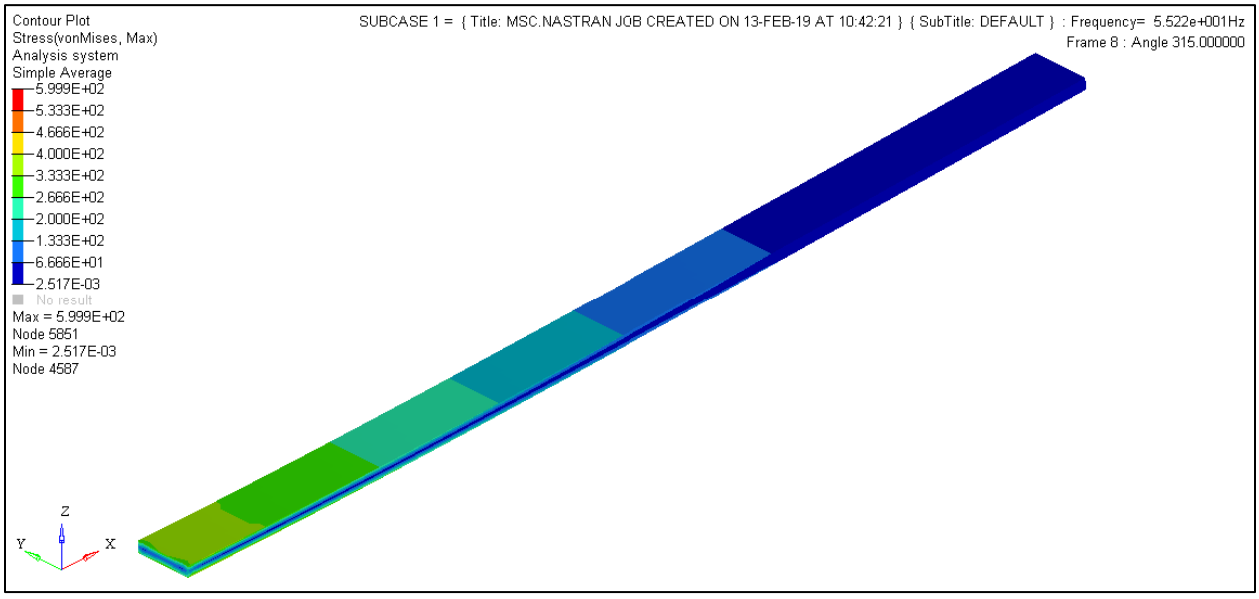

Figure 3-37: Von-Mises Stress at 1st Natural Frequency (Coated beam)

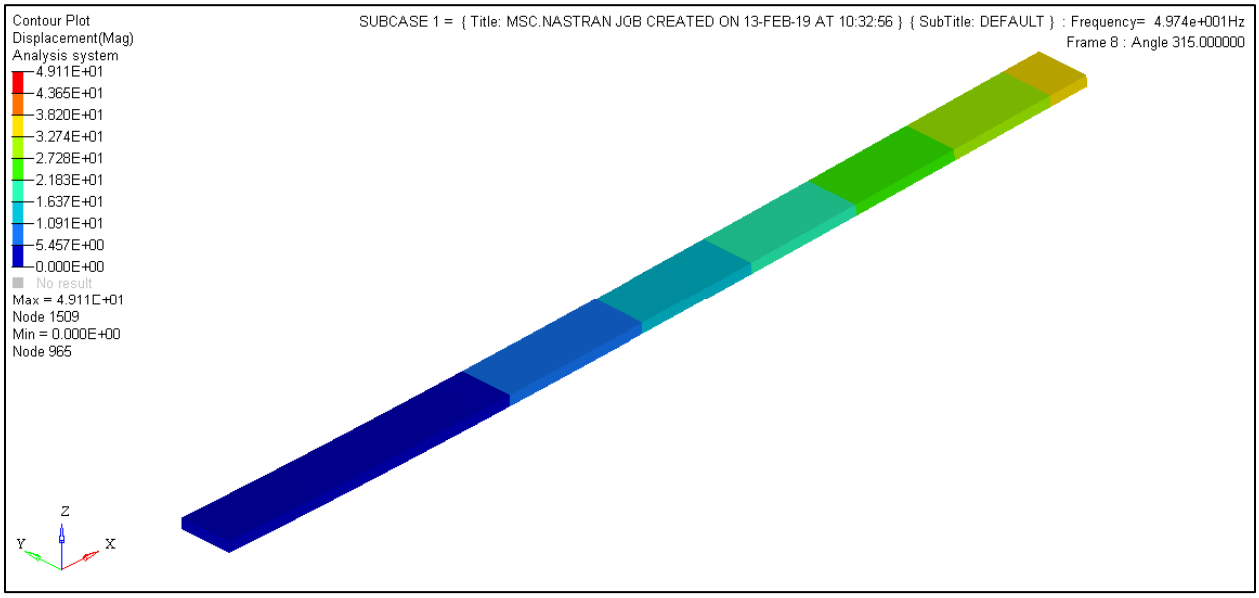

Figure 3-38: Deformation Contours at 1st Natural Frequency (Uncoated beam)

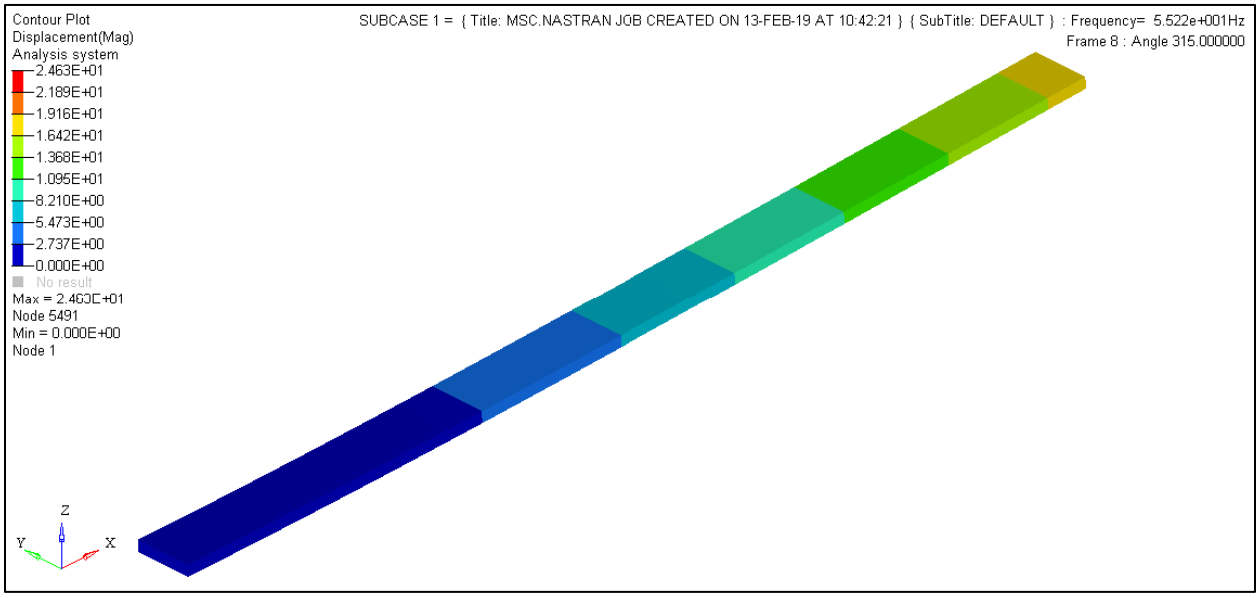

Figure 3-39: Deformation Contours at 1st Natural Frequency (Coated beam)

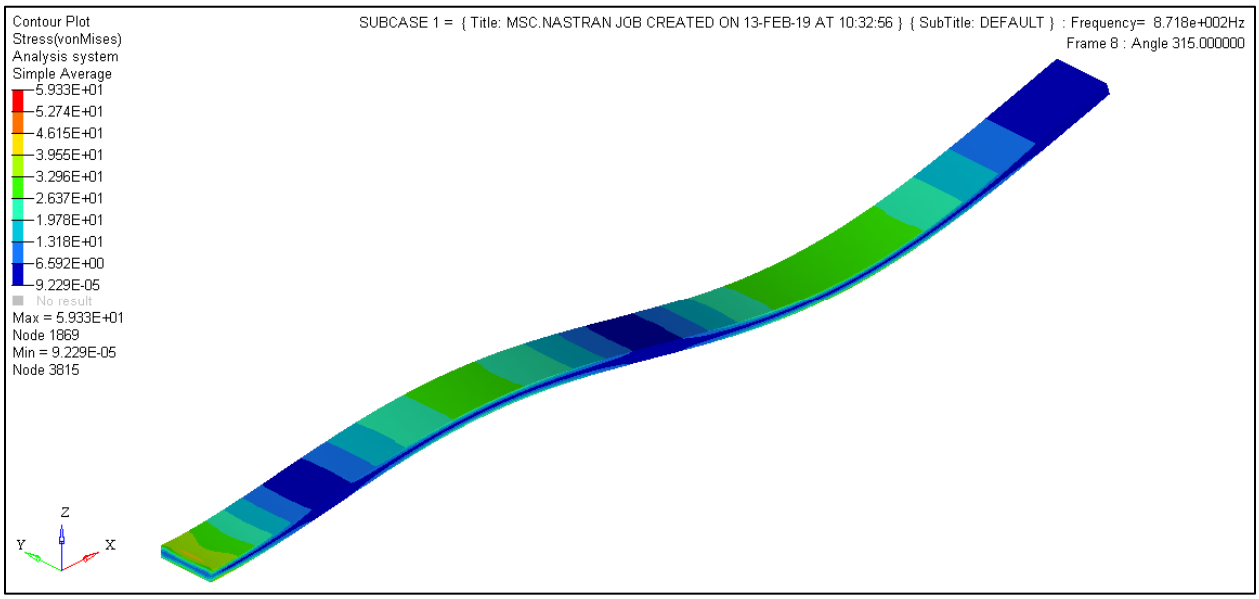

Figure 3-40: Von-Mises Stress at 3rd Natural Frequency (Uncoated beam)

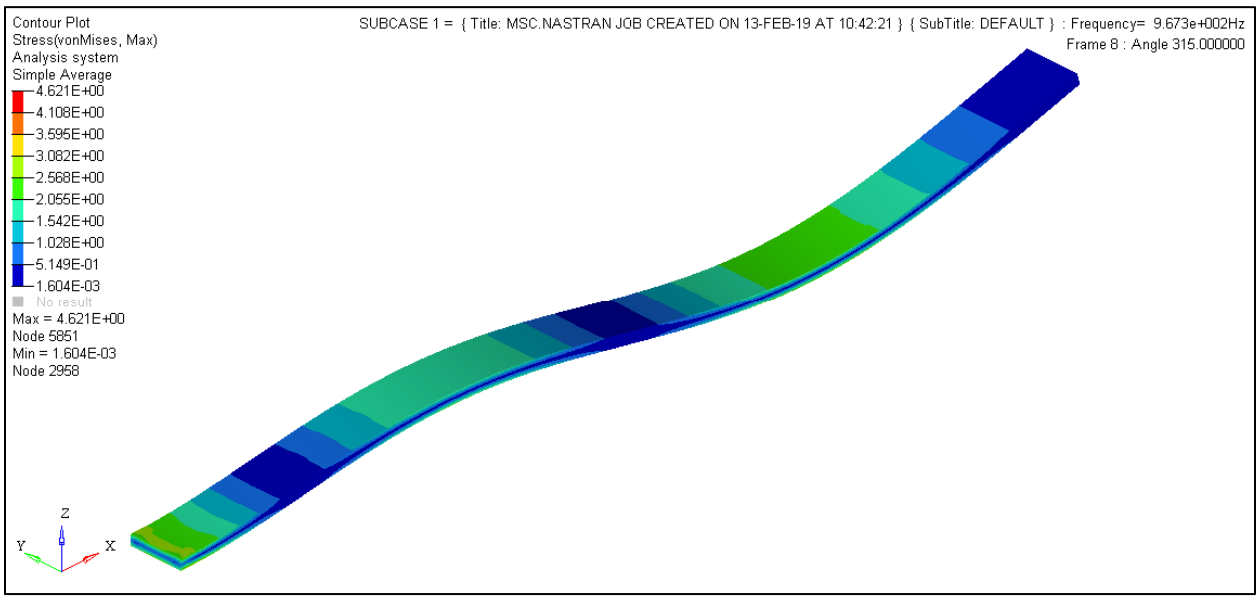

Figure 3-41: Von-Mises Stress at 3rd Natural Frequency (Coated beam)

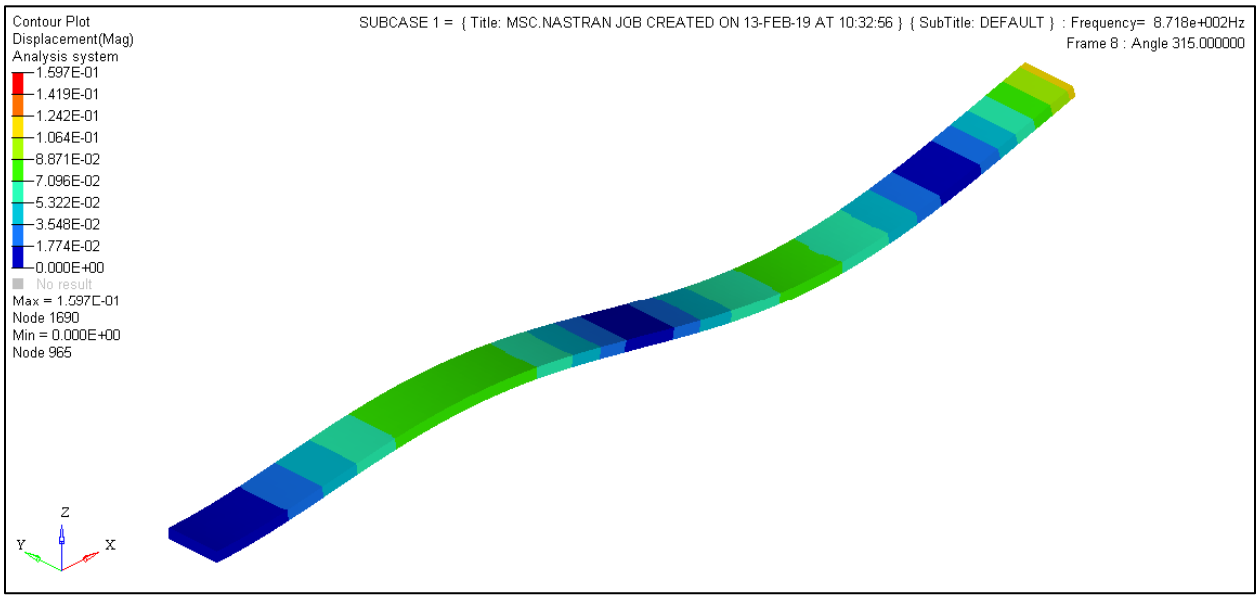

Figure 3-42: Deformation Contours at 3rd Natural Frequency (Uncoated beam)

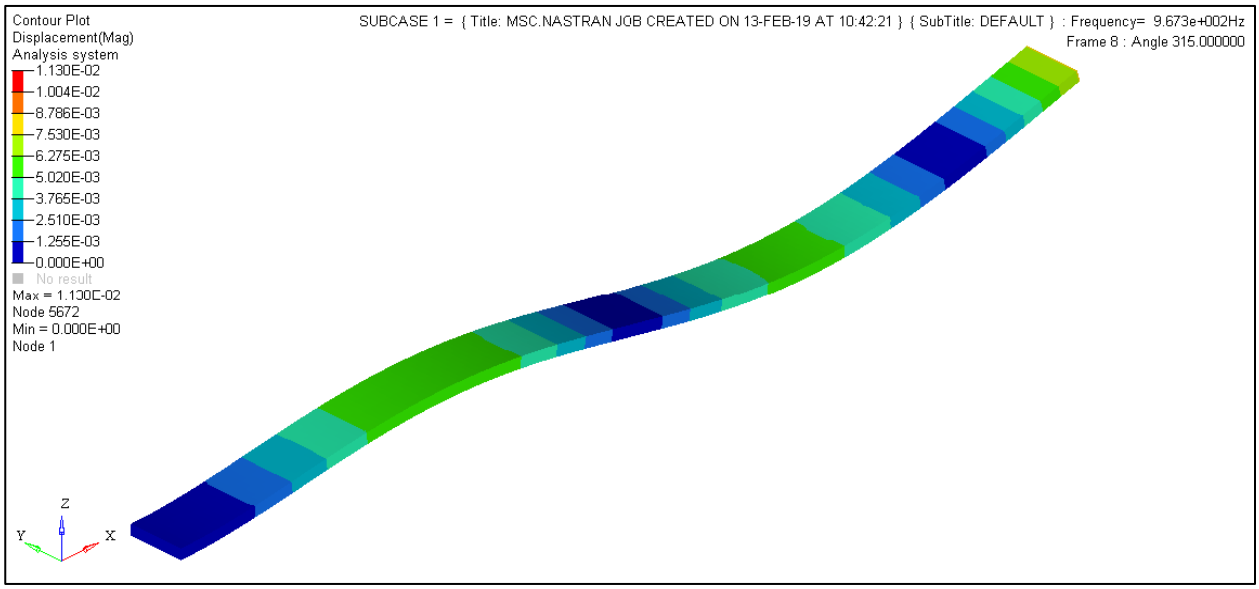

Figure 3-43: Deformation Contours at 3rd Natural Frequency (Coated beam)

3.3 Conclusion

Both the experimental and numerical analysis results show that the coating of 200μm improved the vibration parameters of the beams. And it was more effective in the case of thin beams as compared to thick beams, as maximum improvement was observed in 2mm beam, while least improvement was observed in the case of 3mm beam.

But the percentage change in different parameters before and after coatings was different in each case as shown in table 3-23, and are also presented in figure 3-44.

Table 3-23: Comparison of improvement in Vibration Parameters

Vibration Parameter	Percentage Change
1st Natural Frequency (Experimental)	6.9 - 10.3
Maximum Displacement (Experimental)	17.1 - 49.3
Damping Ratio (Experimental)	15.0 - 44.8
Natural Frequency (Numerical)	7.3 - 11
Maximum Displacement at 1st Natural Frequency (Numerical)	23.6 - 49.8
Von-Mises Stresses at 1st Natural Frequency (Numerical)	18.1 - 44.8
Maximum Displacement at 3rd Natural Frequency (Numerical)	87.2 - 92.9
Von-Mises Stresses at 3rd Natural Frequency (Numerical)	86.3 - 92.2

The results show that in most cases, 15-50% change was observed. While maximum change was observed in the case of von-mises stresses and displacements at 3rd natural frequencies. Which indicates that magneto-mechanical coating is most effective at high frequency modes as compared to low frequencies. Therefore, it is suitable for turbine blades and aircraft engines.

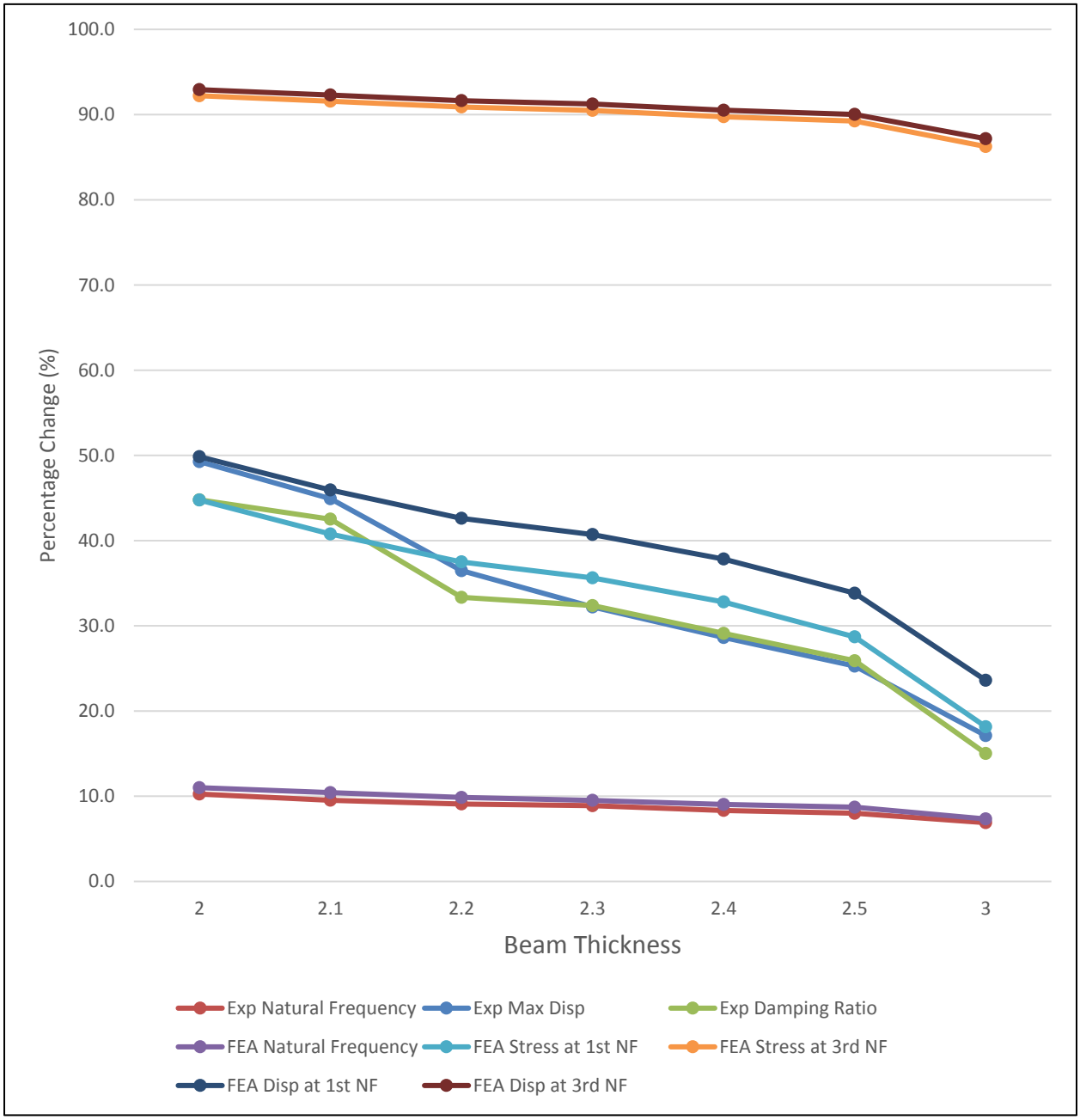

Figure 3-44: Comparison of improvement in Vibration Parameters

CHAPTER 4 : EFFECT OF MAGNETOMECHANICAL COATING THICKNESS IN BEAM STRUCTURES

In this chapter the effect of magnetomechanical coating thickness on a single beam of 180mm x 10mm x 2mm is investigated by applying coatings of different thicknesses (0.05mm-0.3mm) and then finding their damping characteristics both by experiments and through numerical analysis.

4.1 Experimental Work

The same experimental setup as used in chapter 3 was used to find the damping characteristics of the beam. The results are presented as follows:

4.1.1 Natural Frequencies:

The results of natural frequencies of beams are given in table 4-1. And sample result of beam with 0.3mm coating thickness is shown in figure 4-1.

Table 4-1: Natural Frequencies of beams

Coating Thickness (mm)	1st Natural Frequencies		2nd Natural Frequencies		3rd Natural Frequencies	
	Frequency (HZ)	Increase (%)	Frequency (HZ)	Increase (%)	Frequency (HZ)	Increase (%)
Uncoated	48.75	-	266.25	-	762.50	-
0.05	50.00	2.56	281.25	5.63	803.75	5.41
0.1	51.25	5.13	292.50	9.86	830.00	8.85
0.15	52.50	7.69	295.00	10.80	839.99	10.16
0.2	53.75	10.26	306.50	15.12	881.25	15.57
0.25	55.00	12.82	297.50	11.74	845.00	10.82
0.3	56.25	15.38	313.75	17.84	892.50	17.05

The natural frequency results indicate that as we increase the coating thickness the natural frequencies increase. And percentage change in every increase is proportional to the coating thickness as presented in figure 4-2.

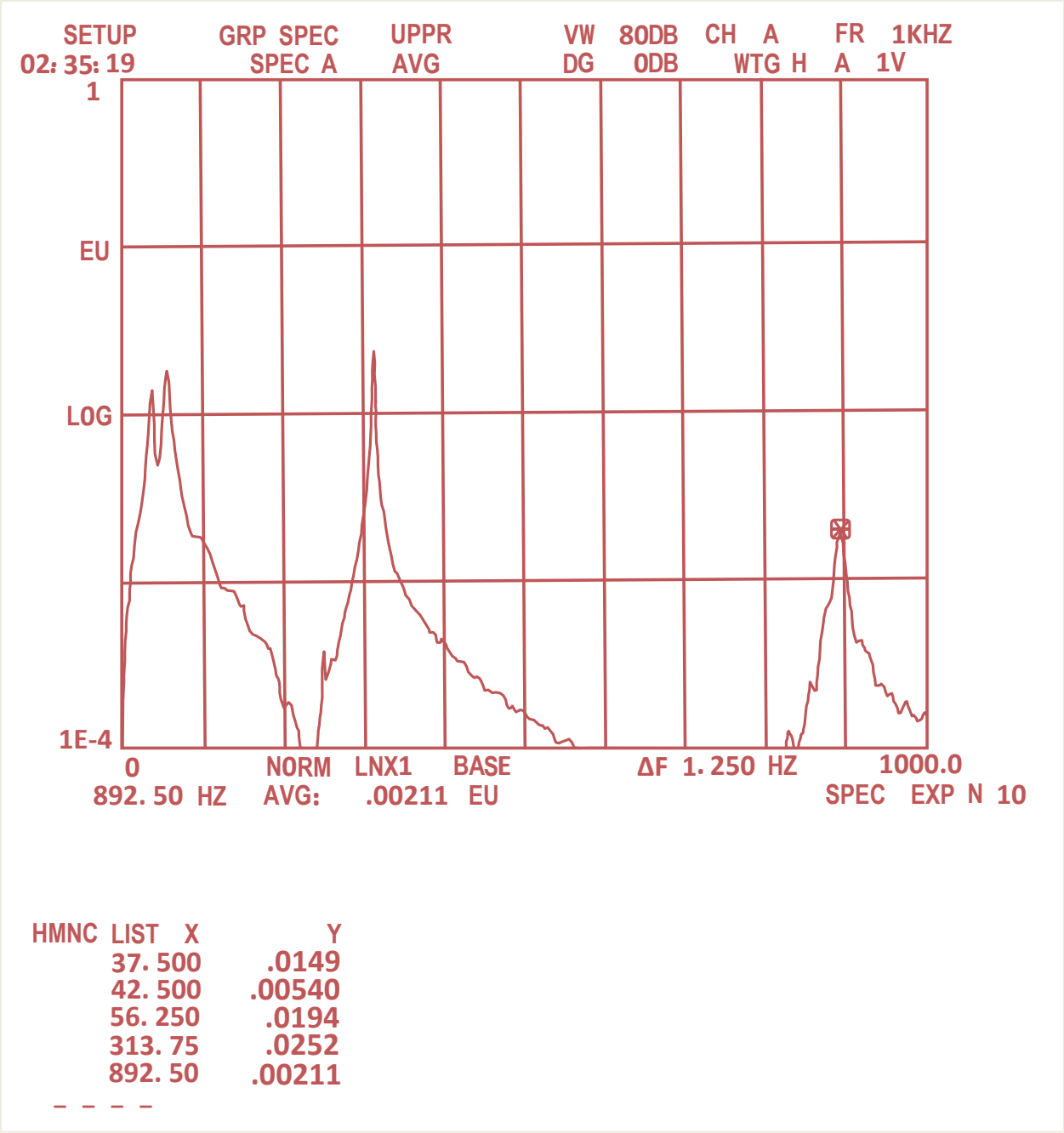

Figure 4-1: Natural Frequencies of Beam (beam with 0.3mm Coating)

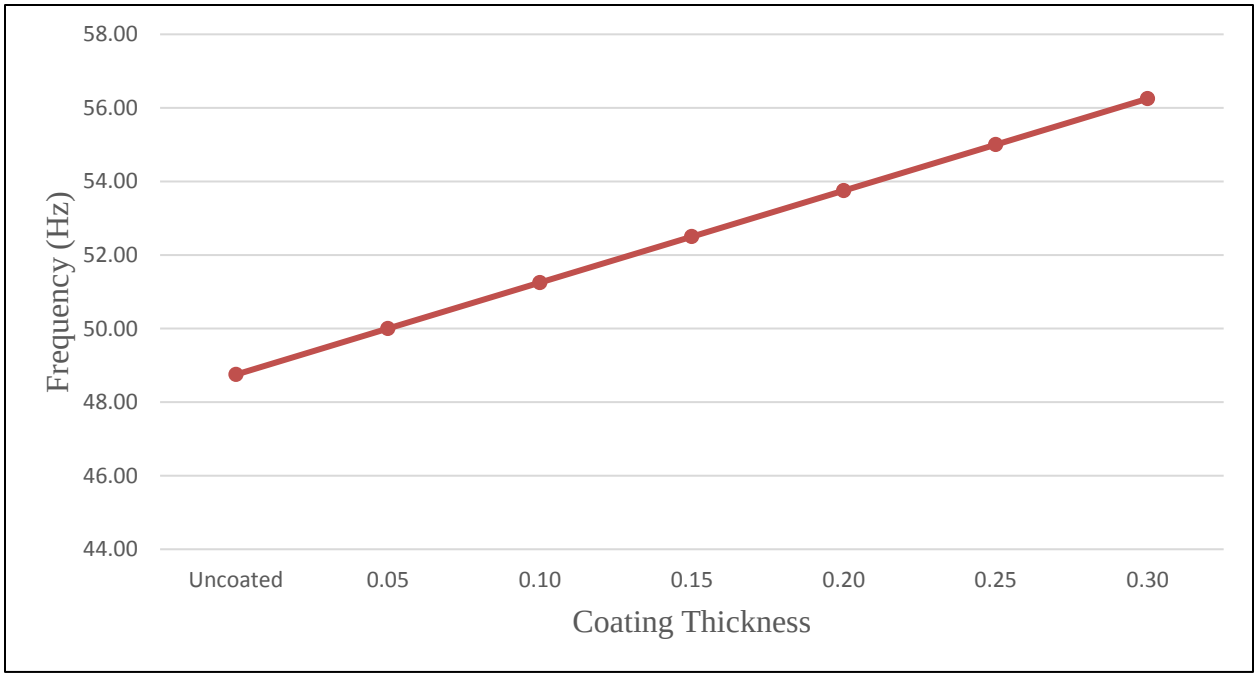

Figure 4-2: 1st Natural Frequencies of Beams

4.1.2 Maximum Displacement

The Results of the experiments are given in table 4-2. And sample results of beam with 0.3mm coating is shown in figure 4-3.

Table 4-2: Maximum Displacement of beams at 1st Natural Frequencies

Beam	Maximum Displacement	% Decrease
Uncoated	20.7	-
0.05	12.2	41.1
0.10	11.6	44.0
0.15	11.1	46.4
0.20	10.5	49.3
0.25	9.9	52.2
0.30	9.3	55.1

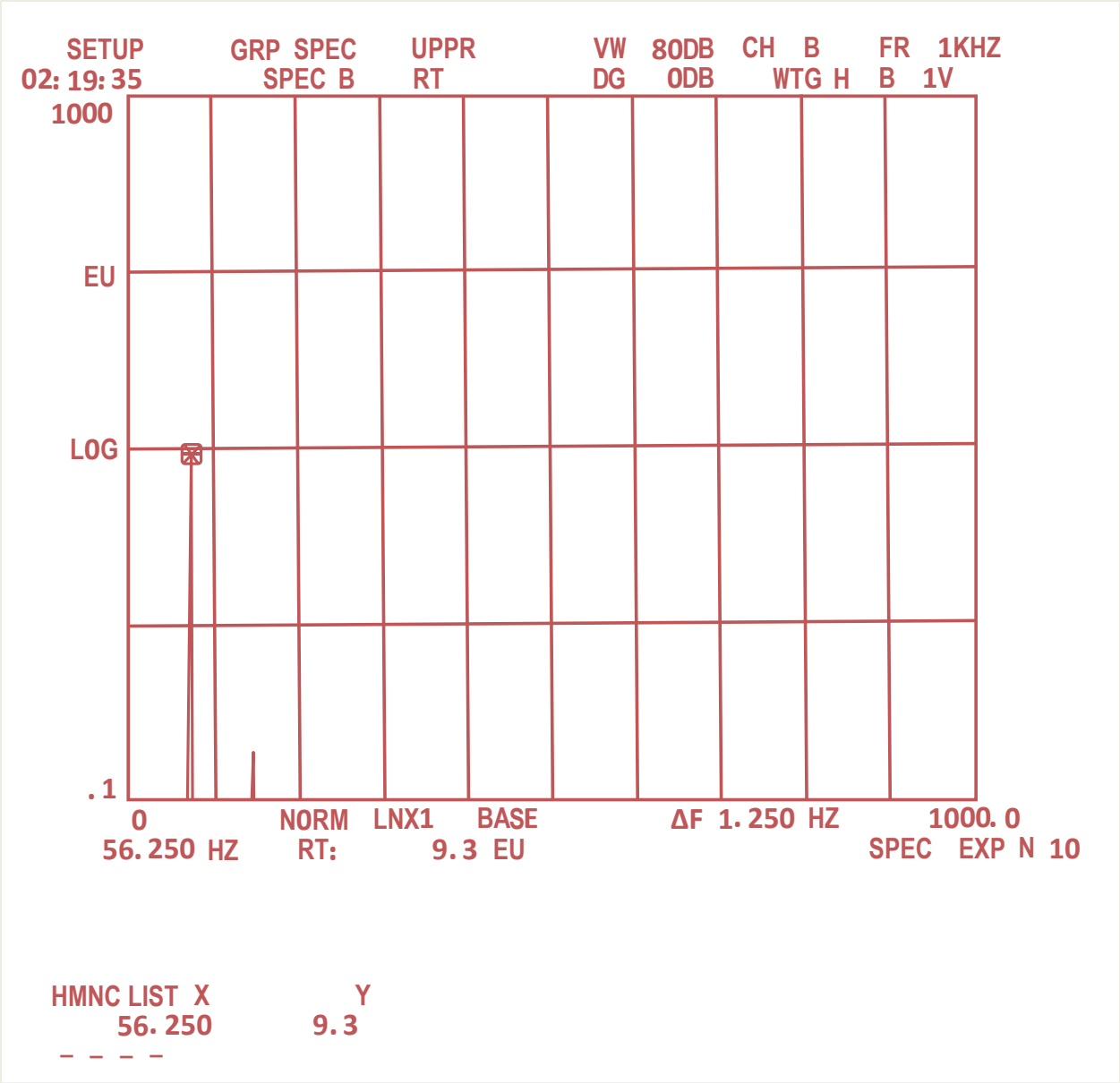

Figure 4-3: Maximum Displacement of Beam (beam with 0.3mm Coating)

The results indicate that as we increase the coating thickness the maximum displacement is decreased. And percentage change in every decrease is proportional to the coating thickness as presented in figure 4-4.

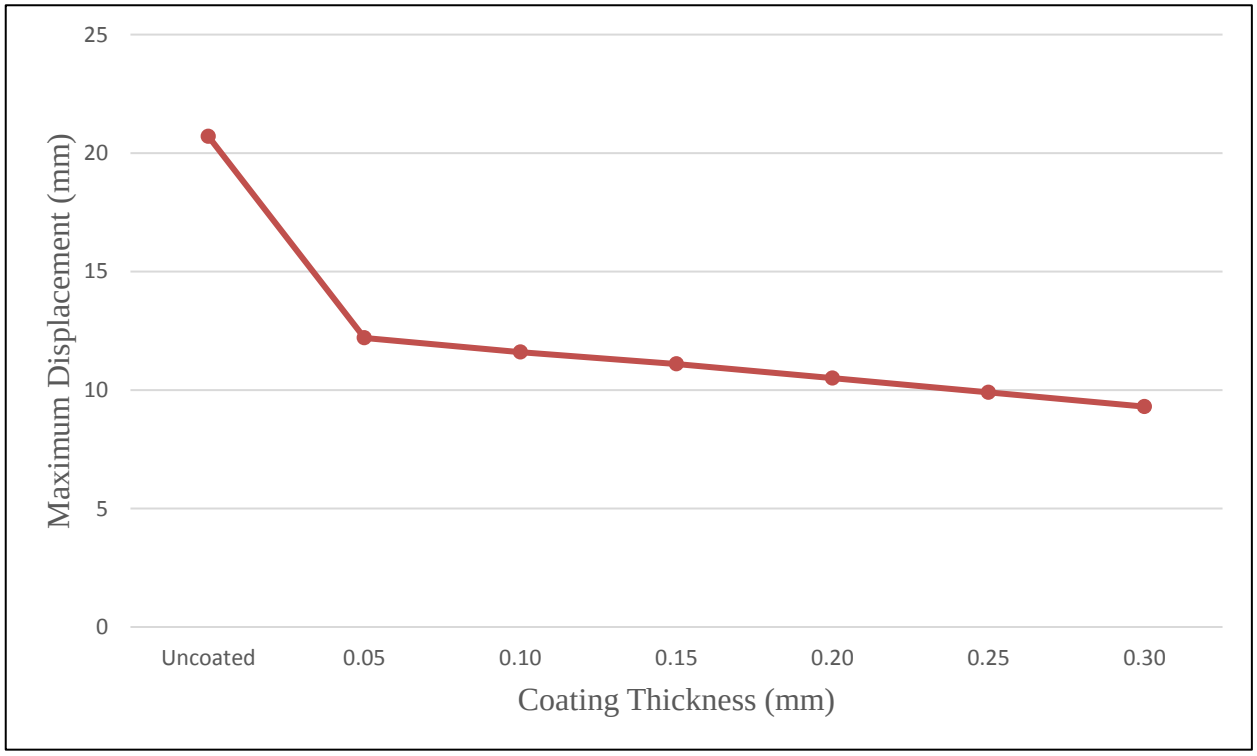

Figure 4-4: Maximum Displacement in Beams

4.1.3 Damping Ratio:

The Damping ratios of coated beams are given in table 4-2. And sample time domain response of beam with 0.3mm coating is shown in figure 4-5.

Table 4-3: Damping Ratios of Beams

Coating Thickness (mm)	Damping Ratio	% Increase
Uncoated	0.0097	-
0.05	0.0119	22.2
0.1	0.0123	26.1
0.15	0.0132	35.1
0.2	0.0141	44.8
0.25	0.0148	51.7
0.3	0.0156	59.8

The results indicate that as we increase the coating thickness the damping ratio increases. And percentage change in every decrease is proportional to the coating thickness as presented in figure 4-6.

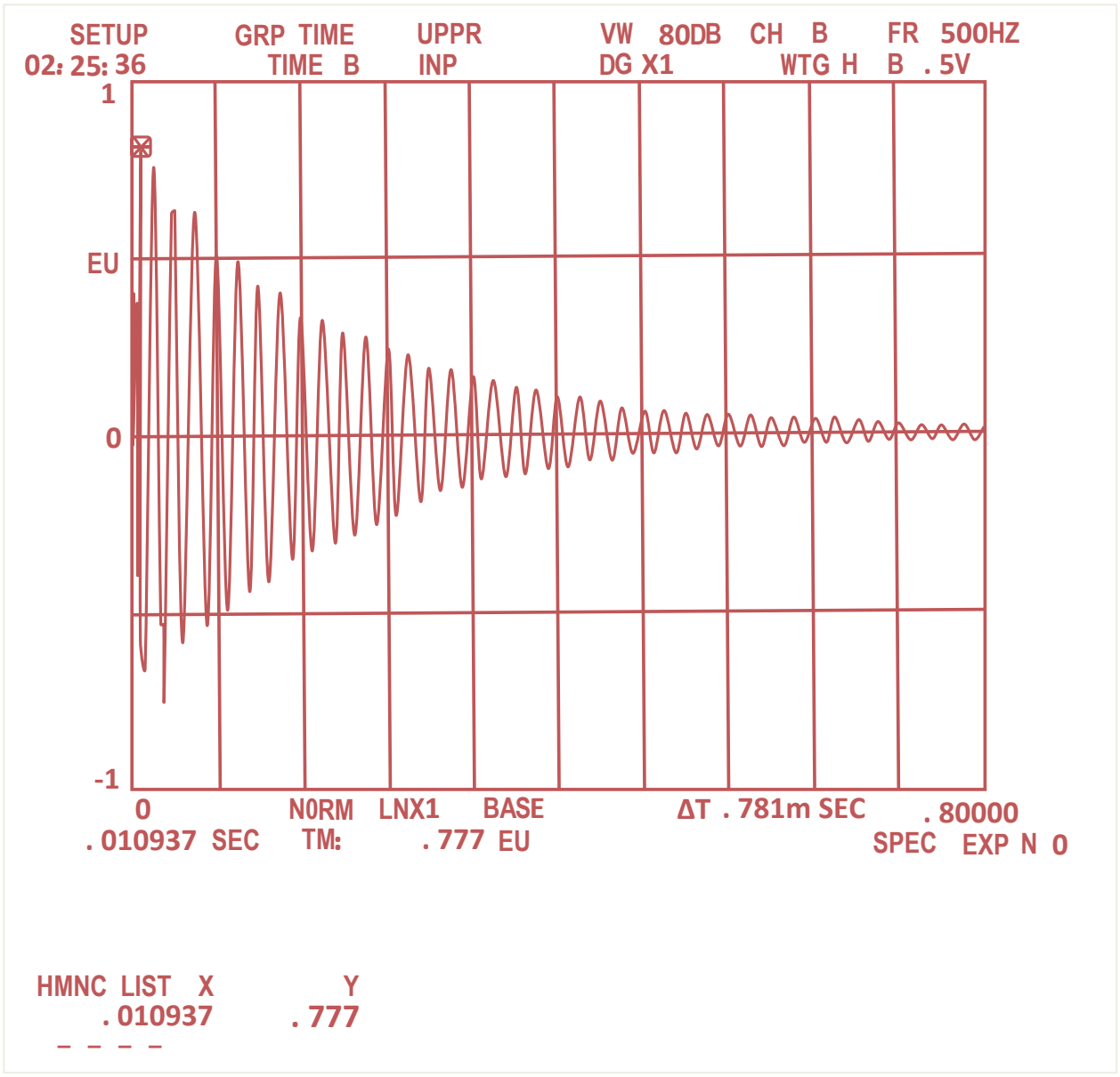

Figure 4-5: Time domain response of Beam (with 0.3mm Coating)

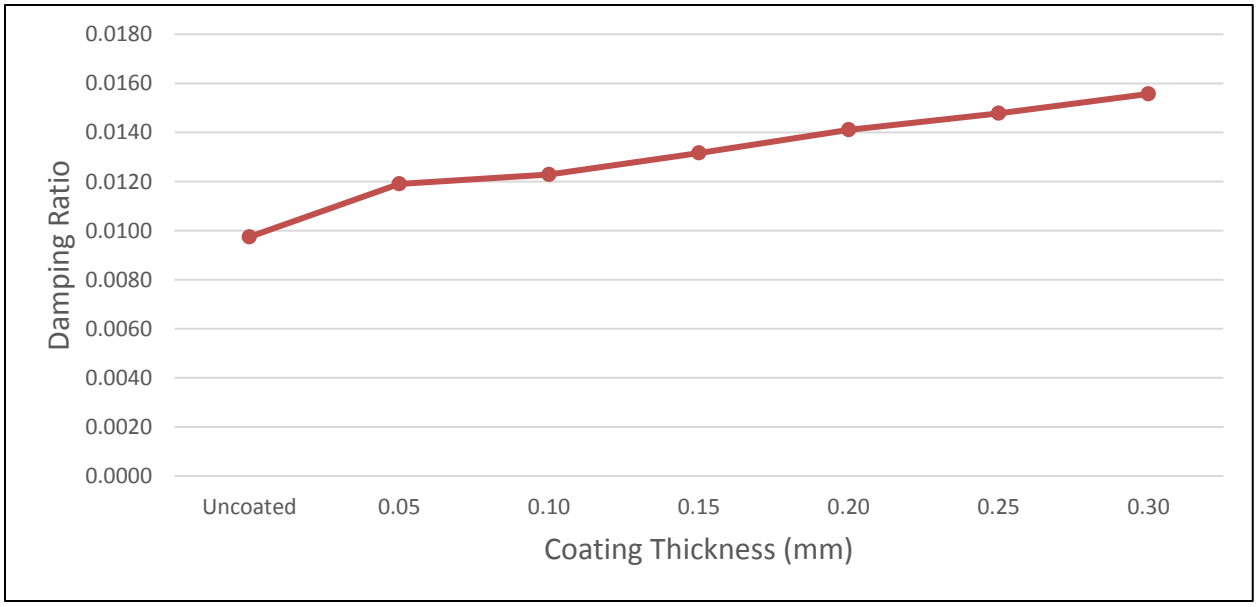

Figure 4-6: Damping Ratios of Beams

4.2 Numerical Analysis

4.2.1 Modal Analysis

Modal analysis was performed to find the mode shapes and natural frequencies of all the beams.

4.2.1.1 Natural Frequencies of beams

Natural Frequencies of uncoated and coated beams are shown in table 4-4. Only 1st and 3rd bending modes are considered in this analysis.

Table 4-4: Natural Frequencies of beams

Coating Thickness (mm)	Frequency [Hz]		% Increase
	1st	3rd	
Uncoated	49.74	871.76	-
0.05	51.12	895.72	2.8
0.1	52.49	919.64	5.5
0.15	53.85	943.50	8.3
0.2	55.22	967.32	11.0

0.25	56.58	991.10	13.7
0.3	57.94	1014.90	16.5
0.35	59.30	1038.60	19.2
0.4	60.66	1062.30	21.9
0.45	62.01	1085.90	24.7
0.5	63.37	1109.60	27.4

The natural frequency results indicate that as we increase the coating thickness the natural frequencies increase. And change in every increase is proportional to the coating thickness as presented in figure 4-7.

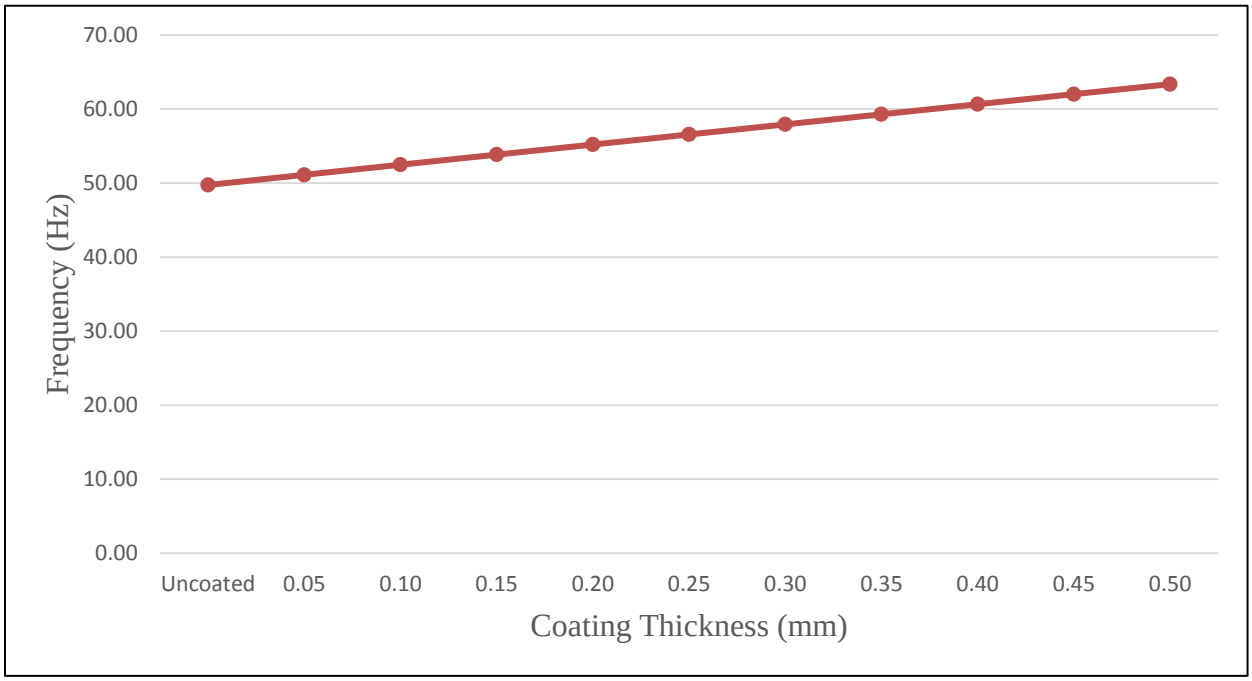

Figure 4-7: Comparison of 1st Natural Frequencies with Different Coating Thicknesses

4.2.2 Harmonic Response

Harmonic response has been obtained by exciting the uncoated and coated beams at 1st and 3rd natural frequencies. The Maximum displacements and Von-Mises stresses of uncoated and coated beams are shown in tables 4-5 to 4-8.

Table 4-5: Von-Mises Stresses at 1st Natural Frequencies

Beam Thickness (mm)	Von-Mises Stress (MPa)	% Reduction
Uncoated	1086.00	-
0.05	673.50	38.0
0.1	651.00	40.1
0.15	626.60	42.3
0.2	599.90	44.8
0.25	571.80	47.3
0.3	541.70	50.1
0.35	509.80	53.1
0.4	476.10	56.2
0.45	438.30	59.6
0.5	398.50	63.3

Table 4-6: Maximum Displacement at 1st Natural Frequency

Beam Thickness (mm)	Maximum Displacement (mm)	% Reduction
Uncoated	49.11	-
0.05	29.69	39.5
0.1	28.01	43.0
0.15	26.32	46.4
0.2	24.63	49.8
0.25	22.96	53.2
0.3	21.28	56.7
0.35	19.61	60.1
0.4	17.93	63.5
0.45	16.18	67.1
0.5	14.43	70.6

Table 4-7: Von-Mises Stresses at 3rd Natural Frequency

Beam Thickness (mm)	Von-Mises Stress (MPa)	% Reduction
Uncoated	59.33	-
0.05	9.48	84.0
0.1	6.59	88.9
0.15	5.33	91.0
0.2	4.62	92.2
0.25	4.17	93.0
0.3	3.80	93.6
0.35	3.52	94.1
0.4	3.32	94.4
0.45	3.17	94.7
0.5	3.03	94.9

Table 4-8: Maximum Displacement at 3rd Natural Frequency

Beam Thickness (mm)	Maximum Displacement (mm)	% Reduction
Uncoated	0.1597	-
0.05	0.0249	84.4
0.1	0.0169	89.4
0.15	0.0133	91.7
0.2	0.0113	92.9
0.25	0.0100	93.8
0.3	0.0089	94.5
0.35	0.0081	94.9
0.4	0.0074	95.3
0.45	0.0070	95.6
0.5	0.0065	95.9

The results show that as we increase the coating thickness, the Von-mises stresses and Maximum displacement at free end of the beam are reduced by ~40-70% at 1st natural frequencies, and was ~84-95% at 3rd natural frequencies. And the decrease is proportional to the coating thickness as shown by graphical plots presented in figures 4-8 to 4-11.

Sample contour plots of 2mm beam with 0.5mm coating are presented in figures 4-12 to 4-15.

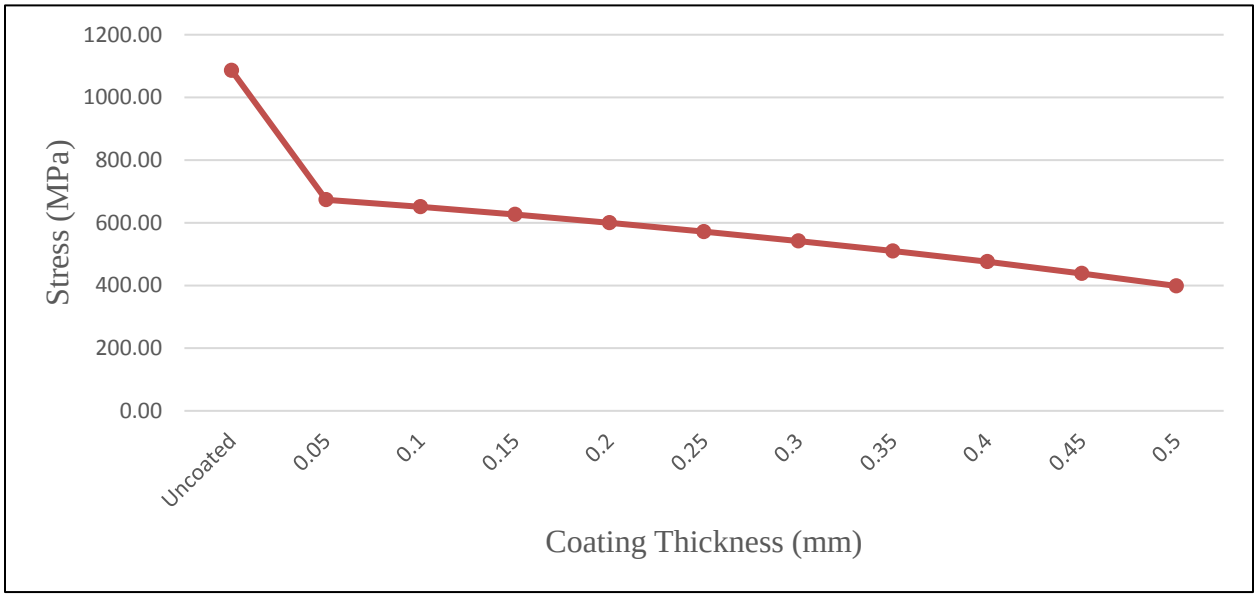

Figure 4-8: Comparison of Von-Mises Stresses at 1st Natural Frequencies

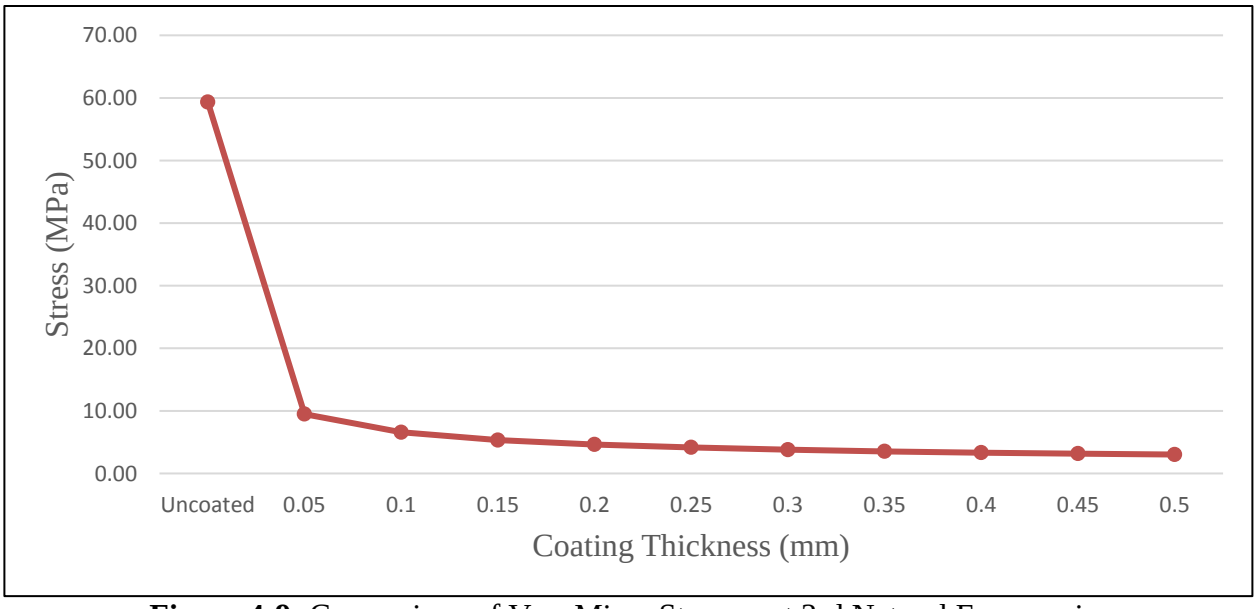

Figure 4-9: Comparison of Von-Mises Stresses at 3rd Natural Frequencies

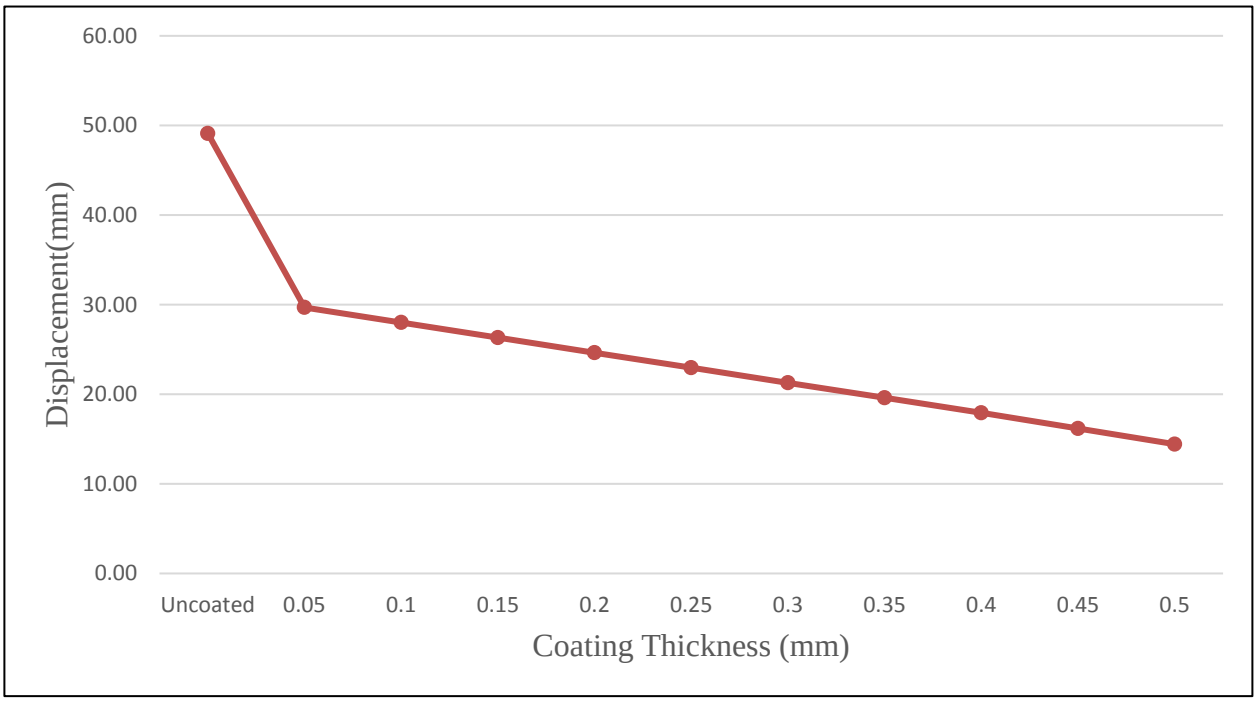

Figure 4-10: Comparison of Maximum Displacements at 1st Natural Frequencies

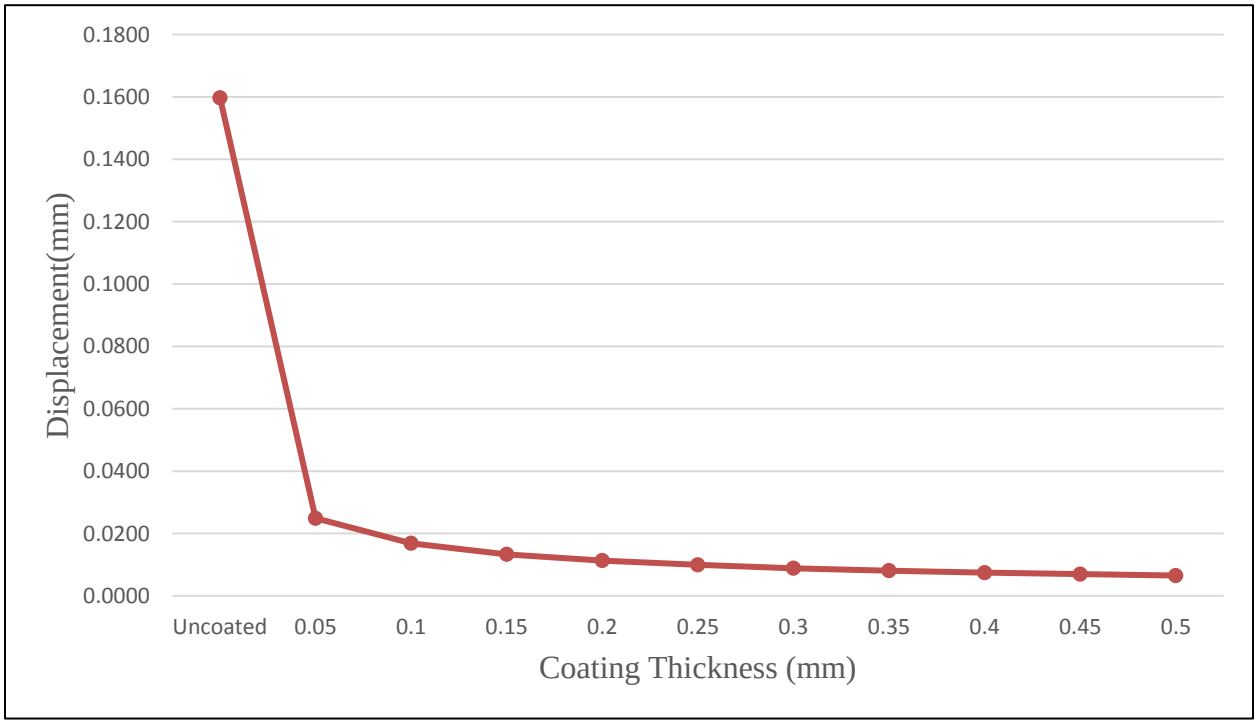

Figure 4-11: Comparison of Maximum Displacements at 3rd Natural Frequencies

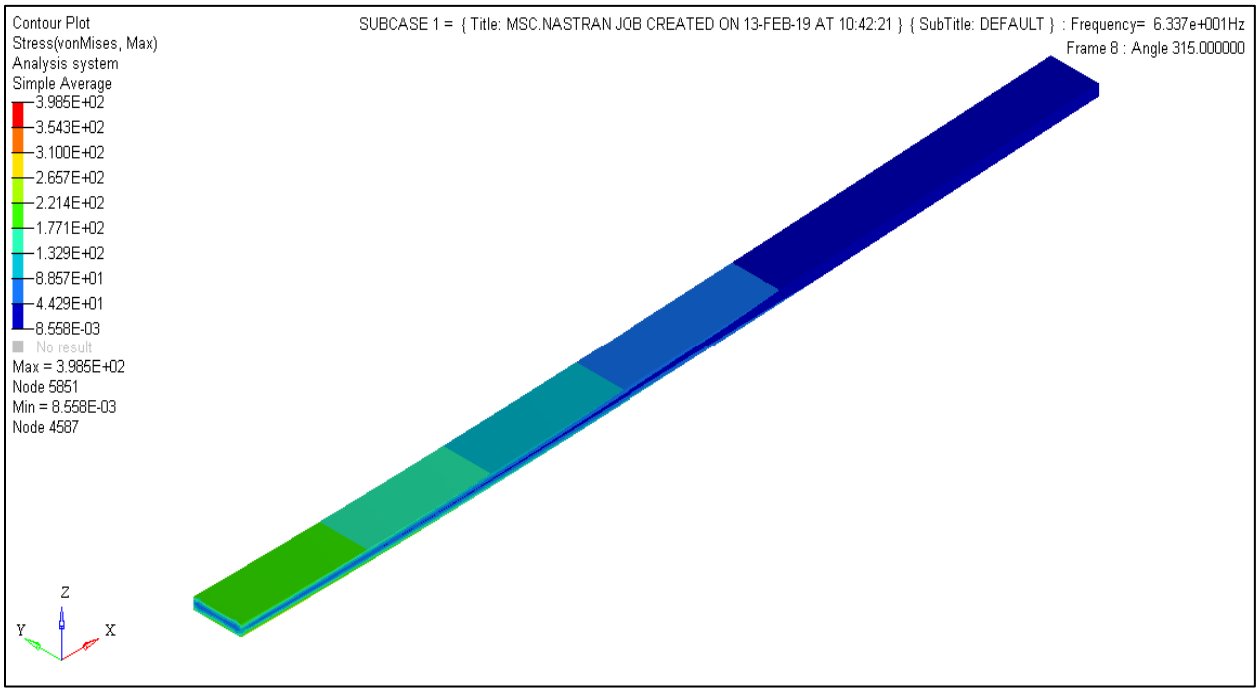

Figure 4-12: Von-Mises Stress at 1st Natural Frequency (beam with 0.5mm Coating)

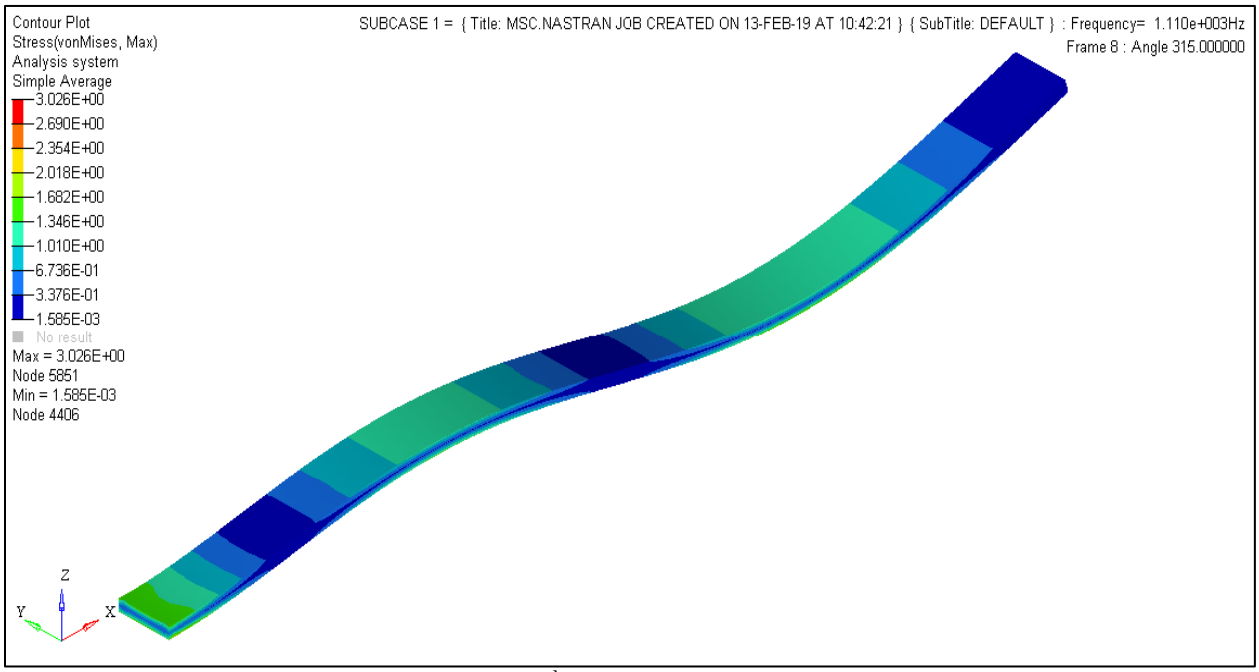

Figure 4-13: Von-Mises Stress at 3rd Natural Frequency (beam with 0.5mm Coating)

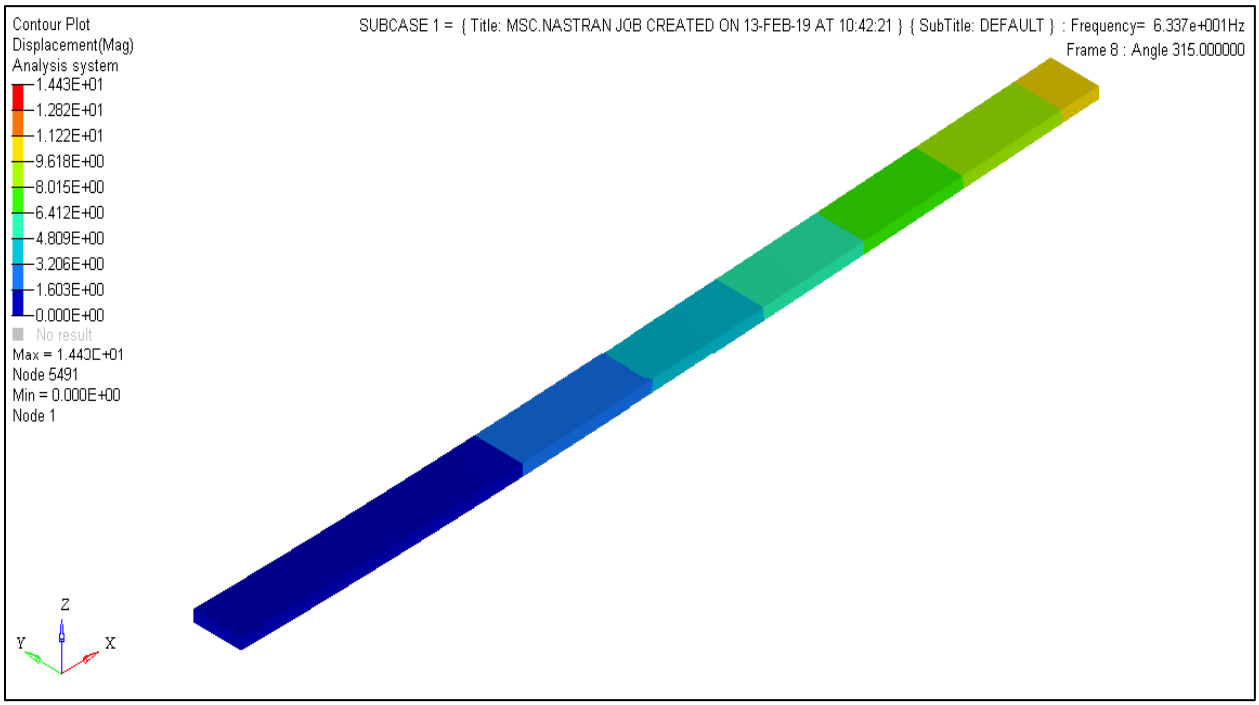

Figure 4-14: Deformation Contours at 1st Natural Frequency (beam with 0.5mm Coating)

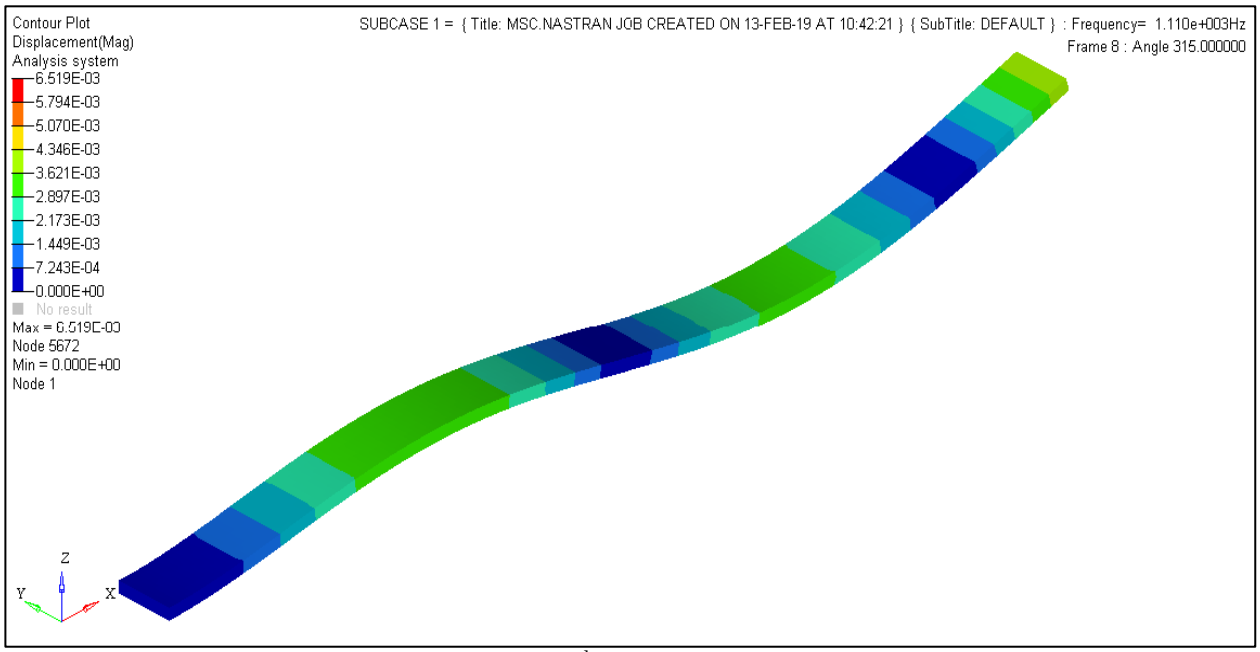

Figure 4-15: Deformation Contours at 3rd Natural Frequency (beam with 0.5mm Coating)

4.3 Conclusion

Both the experimental and numerical analysis results show that as we increase the coating thickness, the vibration parameters are improved. And the improvement is directly proportional to the thickness of the coating. But as thicker coatings have applicability and reliability issues, and are observed to creep under high stresses, therefore, an optimum coating thickness should be used, which is sufficient enough to keep our vibrations under control. As excessive coatings are not cost effective, and are likely to chip off under high vibrations.

The percentage changes in different vibration parameters are shown in table 4-9, and are also plotted in figure 4-16.

The results show that in most cases, 22 - 60% change was observed. While maximum change was observed in the case of von-mises stresses and displacement at 3rd natural frequencies (~85 – 95%). Which indicates that magnetomechanical coating is most effective at high frequency modes as compared to low frequencies. Therefore, it is suitable for turbine blades and aircraft engines.

Table 4-9: Comparison of improvement in Vibration Parameters

Vibration Parameter	Percentage Change
1st Natural Frequency (Experimental)	2.56 – 15.38
Maximum Displacement (Experimental)	41.1 - 55.1
Damping Ratio (Experimental)	22.2 – 59.8
Natural Frequency (Numerical)	2.8 – 16.5
Maximum Displacement at 1st Natural Frequency (Numerical)	39.5 - 56.7
Von-Mises Stresses at 1st Natural Frequency (Numerical)	38 – 50.1
Maximum Displacement at 3rd Natural Frequency (Numerical)	84 – 93.6
Von-Mises Stresses at 3rd Natural Frequency (Numerical)	84.4 - 94.5

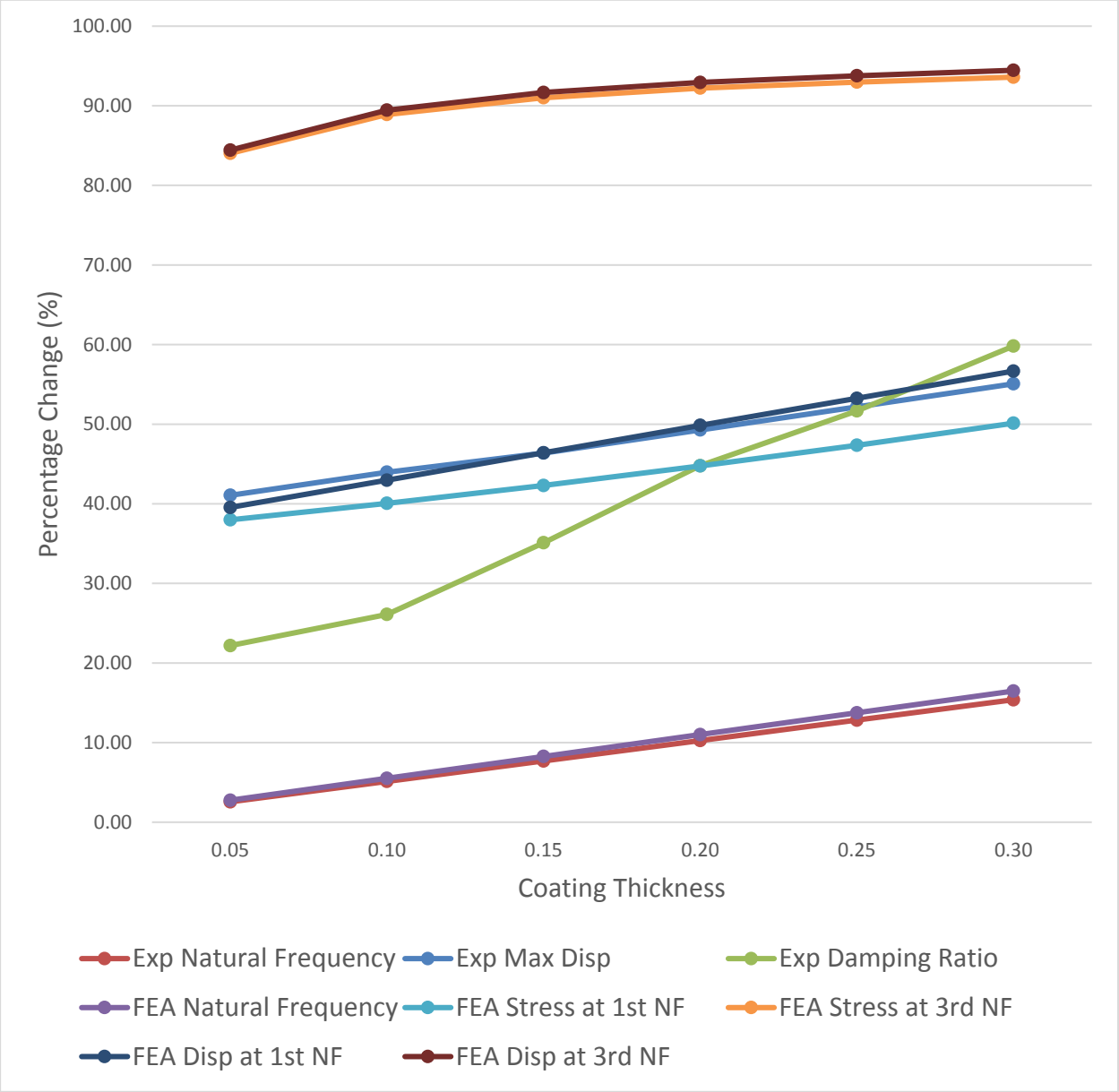

Figure 4-16: Comparison of improvement in Vibration Parameters

REFERENCES

[1] J. H. Griffin, "Friction damping of resonant stresses in gas turbine engine airfoils," *Journal of Engineering for Power*, vol. 102, pp. 329-333, 1980.

[2] R. Gordon, J. Hollkamp, R. Gordon and J. Hollkamp, "An internal damping treatment for gas turbine blades," in *38th Structures, Structural Dynamics, and Materials Conference*, 1997.

[3] R. Kielb, F. Macri, D. Oeth, A. Nashif, P. Macioce, H. Panossian and F. Lieghley, "Advanced damping systems for fan and compressor blisks," in *34th AIAA/ASME/SAE/ASEE Joint Propulsion Conference and Exhibit*, 1998.

[4] J. Hoffman, *Magnetic damping system to limit blade tip vibrations in turbomachines*, Google Patents, 1996.

[5] K. R. Cross, W. R. Lull, R. L. Newman and a. R. Cavanagh, "Potential of graded coatings in vibration damping," *Journal of Aircraft*, vol. 10, pp. 689-691, 1973.

[6] R. Becker and M. Kornetzki, "Effect of Magnetostriction in Ferromagnetic materials," *Z. Physik*, vol. 88, p. 634, 1934.

[7] A. W. Cochardt, "The origin of damping in high-strength ferromagnetic alloys," *JOURNAL OF APPLIED MECHANICS-TRANSACTIONS OF THE ASME*, vol. 20, pp. 196-200, 1953.

[8] G. W. Smith and J. R. Birchak, "Effect of internal stress distribution on magnetomechanical damping," *Journal of Applied Physics*, vol. 39, pp. 2311-2316, 1968.

[9] G. W. Smith and J. R. Birchak, "Internal Stress Distribution Theory of Magnetomechanical Hysteresis-An Extension to Include Effects of Magnetic Field and Applied Stress," *Journal of Applied Physics*, vol. 40, pp. 5174-5178, 1969.

[10] B. J. Lazan, "Material and Structural Damping for Vibration Control," *SAE Transactions*, pp. 537-547, 1960.

[11] D. Kroisová, "Vibration damping in polymer matrix composite systems," *23rd International Conference on Noise and Vibration Engineering 2008, ISMA 2008*, vol. 2, pp. 871-880, 1 2008.

[12] C. Hirunyapruk, "Vibration control using an adaptive tuned magneto-rheological fluid vibration absorber," 2009.

[13] I. Pelinescu and A. Christie, "Measuring Damping Loss Factors of High Performance LASD Coatings," 2011.

[14] F. Ghezzo and X. Miao, "COMPOSITE COATINGS WITH HIGH VIBRATION DAMPING PROPERTIES".

[15] P. J. Torvik, "A survey of the damping properties of hard coatings for turbine engine blades," *Integration of Machinery Failure Prevention Technologies Into System Health Management*, pp. 485-506, 2007.

[16] M.-H. H. Shen, *Free layer blade damper by magneto-mechanical materials*, Google Patents, 2008.

[17] I. Aziz, S. Hussain, W. Tarar and I. Akhtar, "Experimental and Numerical Investigation of Vibration Damping Using a Thin Layer Coating," in *ASME 2017 Power Conference Joint*

With ICOPE-17 collocated with the ASME 2017 11th International Conference on Energy Sustainability, the ASME 2017 15th International Conference on Fuel Cell Science, Engineering and Technology, and the ASME 2017 Nuclear Forum, 2017.

[18] H.-Y. Yen, "New analysis and design procedures for ensuring gas turbine blades and adhesive bonded joints structural integrity and durability," 2000.

[19] I. Aziz, W. Tarar, I. Akhtar and M. N. Azam, "Vibratory Stress Suppression in Turbine Blades Subjected to Aerodynamic Loading," in *ASME 2013 International Mechanical Engineering Congress and Exposition*, 2013.

[20] S. H. Raza, M. A. Malik and W. Akram, "Analysis of material coating for damping in beam structures," in *Key Engineering Materials*, 2010.

[21] N. Good, J. Dooley and B. Fultz, "Magnetomechanical damping by polycrystalline TbDy," *Journal of applied physics,* vol. 91, pp. 7824-7826, 2002.

[22] K. B. Hathaway, A. E. Clark and J. P. Teter, "Magnetomechanical damping in giant magnetostriction alloys," *Metallurgical and Materials Transactions A,* vol. 26, pp. 2797-2801, 1995.

[23] D. W. Shoon, C. Y. Kang, K. Miyahara and J. H. Sung, "Effect of Microstructure on the Damping Capacity and Strength in Fe-Al-Mn Alloy," 2004.

[24] F. Yin, K. Nagai, K. Watanabe and K. Kawahara, "The damping behavior of Ni added Mn-Cu damping alloys," *Materials Transactions,* vol. 44, pp. 1671-1674, 2003.

[25] C. Azcoïtia and A. Karimi, "Magnetomechanical damping in Fe--Cr alloys and effect of Al and Mo addition," *Journal of alloys and compounds,* vol. 310, pp. 160-164, 2000.

[26] V. F. Coronel and D. N. Beshers, "Magnetomechanical damping in iron," *Journal of applied physics,* vol. 64, pp. 2006-2015, 1988.

[27] X. Lu, F. Chen, W. Li and Y. Zheng, "Effect of Ce addition on the microstructure and damping properties of Cu--Al--Mn shape memory alloys," *Journal of Alloys and Compounds,* vol. 480, pp. 608-611, 2009.

[28] R. Lin, W. Jin, M. Cao and R. Yang, "Internal Stress Distribution Model of the Magnetomechanical Hysteresis of Fe-Cr-Al Based Alloys," *Journal of Materials Science & Technology,* vol. 27, pp. 471-474, 2011.

[29] A. Karimi, P. H. Giauque and J. L. Martin, "Magnetomechanical damping in plasma sprayed iron--chromium based coatings," *Journal of applied physics,* vol. 79, pp. 1670-1677, 1996.

[30] R. C. Frank and J. W. Ferman, "Magnetomechanical Damping in Iron—Silicon Alloys," *Journal of Applied Physics,* vol. 36, pp. 2235-2242, 1965.

[31] J. T. A. Roberts and P. Barrand, "Magnetomechanical damping behaviour in pure nickel and a 20 wt.% copper-nickel alloy," *Acta metallurgica,* vol. 15, pp. 1685-1692, 1967.

[32] B. A. Potekhin, S. G. Lukashenko and S. P. Kochugov, "Effect of plasma coatings on the damping properties of structural steels," *Metal science and heat treatment,* vol. 42, pp. 407-410, 2000.